Modifying soil properties with herbaceous plants for natural flood risk-reduction

Boldrin, David; Knappett, Jonathan A.; Leung, Anthony K.; Brown, J. L.; Loades, Kenneth W.; Bengough, A. G.

Published in:
Ecological Engineering

DOI:
10.1016/j.ecoleng.2022.106668

Publication date:
2022

Ecological Engineering 180 (2022) 106668

Contents lists available at ScienceDirect

Ecological Engineering

journal homepage: www.elsevier.com/locate/ecoleng

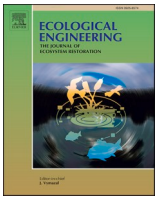

Modifying soil properties with herbaceous plants for natural flood risk-reduction

D. Boldrin [a,b,*], J.A. Knappett [b], A.K. Leung [c], J.L. Brown [a], K.W. Loades [a], A.G. Bengough [a,b]

[a] The James Hutton Institute, Invergowrie, Dundee DD2 5DA, UK
[b] School of Science and Engineering, University of Dundee, Dundee DD2 5DA, UK
[c] Department of Civil and Environmental Engineering, School of Engineering, Hong Kong University of Science and Technology, Clear Water Bay, Kowloon, Hong Kong

ARTICLE INFO

Keywords:
Bioretention
Flood mitigation
Herbaceous species
Nature-based solutions
Soil hydrology
Soil-plant interactions
Root systems

ABSTRACT

Background and aim: Nature-based solutions to engineering challenges are essential to limit climate change impacts on the urban environment. Quantitative understanding of multiple "engineering functions" provided by soil-plant interactions of different species is needed for species selection and re-establishing natural processes affected by urbanisation.

Methods: Contrasting herbaceous species (legumes, grasses, and forbs) were selected and grown as monoculture or species mix in soil columns for a five-month growing season. Saturated hydraulic conductivity was initially tested for each column, and then the columns were monitored for three-weeks of evapotranspiration. Water loss, matric suction, and penetrometer resistance were measured. Finally, soil was tested for aggregate stability and water retention.

Results: Saturated hydraulic conductivity of vegetated soil was generally larger than that of fallow soil ($6.9e^{-6} \pm 1.4e^{-6}$ m/s in fallow soil). Saturated hydraulic conductivity was significantly different between species (e.g., from $9.9e^{-6} \pm 1.3e^{-6}$ m/s in *Festuca ovina* to $3.9e^{-5} \pm 1.2e^{-6}$ m/s in *Lotus corniculatus*) and was negatively correlated with specific root length. The water stored in the soil was efficiently removed by plant transpiration (> 60% of evapotranspiration). Large changes in soil structure were observed in vegetated soil, with significant increases in soil strength, aggregate stability, and alteration of water retention properties.

Conclusions: Multiple soil-plant interactions influence species selection for optimising nature-based solutions (e.g., bioretention barriers). Substantial scope exists to choose species mixes to manipulate soil hydro-mechanical properties. Enhanced biodiversity did not compromise the engineering services of nature-based solutions (e.g., water removal), and may have multiple benefits.

1. Introduction

Climate change is expected to introduce increasing threats to human health and the urban built environment, due to extreme events such as heavy precipitations. A recent study conducted by Bastin et al. (2019) on future climate projections (i.e., to 2050) for 520 major cities, highlighted that 22% of cities will experience extreme climate conditions that are not currently experienced by any existing major city. In North-Europe annual precipitation has increased up to 70 mm per decade from 1950 (Kovats et al., 2014). Climate change predictions highlight that future city growth and projected increases in heavy rainfall events, both together and alone, will lead to increased flood risk (Semadeni-Davies et al., 2008). Conventional stormwater management is primarily designed to mitigate flood risk by quickly directing and discharging runoff water to the drainage system (grey infrastructure). Therefore, stormwater management in the built environment is disconnected from the natural water cycle and experiences high fluctuations of surface water, which can increase downstream flood risk (Marzluff et al., 2008). In recent years, nature-based solutions, such as sustainable drainage systems (SuDS) have been promoted to re-establish natural hydrological processes (e.g., evapotranspiration) which have been removed by urbanisation (Chen et al., 2021; Gimenez-Maranges et al., 2020). In these systems, storm water is managed by slowing down and decreasing the quantity of runoff in the built environment and hence reducing both local and downstream flood risk (CIRIA, 2016). This is achieved by harvesting, infiltrating, slowing, storing, and conveying runoff on site.

* Corresponding author.
E-mail address: david.boldrin@hutton.ac.uk (D. Boldrin).

https://doi.org/10.1016/j.ecoleng.2022.106668
Received 11 October 2021; Received in revised form 7 April 2022; Accepted 20 April 2022
Available online 13 May 2022

In contrast with grey infrastructure (i.e., traditional drainage systems), these nature-based solutions, including bio-retention systems, green roofs, swales and man-made wetlands, can deliver multiple benefits such as increasing resilience to climate change, and encourage biodiversity and habitat connectivity (CIRIA, 2016). Field monitoring of bioretention systems (rain gardens and swales) found that runoff decreased up to 98% (Jiang et al., 2017), although runoff can vary greatly with the intensity and return period of rainfall events.

The use of vegetation in engineering solutions (i.e., nature-based solutions) is now recognised as an effective strategy to mitigate the adverse effects of climate change within the built environment (Tang et al., 2018). Vegetation is a fundamental component of all bioretention systems. Indeed, vegetation is one of the main drivers of the water cycle (Wei et al., 2017). This makes rooted soil one of the most hydrologically dynamic regions of both the pedosphere and biosphere (Bengough, 2012). Roots do not only depend on soil for the acquisition of resources such as water and nutrients; instead they actively engineer soil, changing its physical and chemical properties (Bengough, 2012; Carminati et al., 2010; Tisdall and Oades, 1979). Plant roots influence soil structure through a variety of mechanisms including penetration, anchorage, water uptake, and the exudation of mucilage into the rhizosphere (Jin et al., 2017). For instance, soil shear strength increases with increasing root density (Loades et al., 2010). Furthermore, contrasting root systems can modify soil structure and induce distinctive soil pore changes with coarse roots increasing macro-porosity (Bodner et al., 2014).

In nature-based solutions (e.g., soil bioengineering), rooted soil represents a composite material with enhanced mechanical (Boldrin et al., 2020; Liang et al., 2017), as well as hydrological and hydraulic properties (Leung et al., 2018; Pollen-Bankhead and Simon, 2010). However, plant species can largely differ in terms of the engineering functions they provide (Boldrin et al., 2017; Liang et al., 2017). Moreover, a needed function in one nature-based solution may be useless or detrimental in another one. For example, root-induced changes in soil hydraulic conductivity may play a positive role in “rain gardens” but be potentially detrimental for slope stabilisation (soil bioengineering) and negligible in the shallow and highly permeable substrate of green roofs. A large body of literature exists on plant function and screening for nature-based solutions such as soil reinforcement by bioengineering (Boldrin et al., 2017; De Baets et al., 2007; Ghestem et al., 2014) and green roofs (Seyedabadi et al., 2021). These studies generally focus on one “engineering function” such as water removal (Boldrin et al., 2017) or mechanical reinforcement by root intrusion (De Baets et al., 2007). However, a quantitative understanding of multiple “engineering functions” provided by different species (i.e., different co-occurring soil-plant interactions) is lacking, although needed to guide species screening and finally re-establish natural processes removed by urbanisation. In particular, this is a key step in the design and implementation of new engineered-earth barrier systems for reducing flood risk upon future climate extremes (Petalas et al., 2021). Indeed, the engineering services provided by plants on earth-barrier systems have not been investigated yet. These barrier systems will have to resist extreme events (e.g., flow erosion), allow fast infiltration of rainwater (i.e., stop runoff), retain water (i.e., maximise water holding capacity) and then recharge its water holding capacity (i.e., evapotranspiration of retained water). Vegetation has the potential to drive or maximise all these key features of a barrier system.

This study aims to investigate the effect of contrasting herbaceous species and communities (species mix) in terms of soil-plant interactions that can drive or maximise the multiple functions of a barrier system for flood mitigation. It is hypothesised that (i) vegetated soil with herbaceous species has greater hydraulic conductivity than fallow soil; (ii) species differ in their effect on hydraulic properties; (iii) transpiration can quickly recharge the water-storage capacity of soil; (iv) root intrusion can influence soil water retention properties and porosity; (v) biodiverse vegetation can maximise engineering functions. The experiments reported in this study tested these hypotheses using contrasting herbaceous species (i.e., different functional types), which are widespread in Europe.

2. Materials and methods

2.1. Soil columns

PVC drainage pipes (100 mm inner diameter and 0.5 m long) were used as containers for fallow and vegetated soil columns. The pipes were lined with a 0.2 mm thick polythene sheet to facilitate the extraction of the entire soil columns at the end of the experiment. Before lining the pipes with the polythene sheet, a fine layer of silicon grease was added to the pipe internal wall to improve the sheet adhesion to the pipe as well as stop any potential preferential water flow between the pipe wall and the polythene sheet during irrigation and testing. The base of each pipe was covered with a nylon mesh (1 mm aperture) and an overlying layer of pea gravel (50 mm thick ≈ 650–700 g) to facilitate drainage.

The soil tested in this study was collected from Bullionfield at The James Hutton Institute (Dundee, UK) in March 2019. After collection, soil was air-dried for a week and sieved at 2 mm. This soil can be classified as silt loam, with 43.3% sand, 55.2% silt and 1.5% clay (BS1377). The liquid limit of the soil was 32%, while the plastic limit was 24%, resulting in a low plasticity soil (plasticity index = 8%).

The soil at its optimum water content for compaction (0.18 g/g) was dynamically packed in eight layers of 50 mm height each (393 cm^3 per layer) to obtain a 0.4 m soil column. Each layer was compacted by five blows (7 J per blow) of a standard Proctor hammer (2400 g), targeting a final dry density equal to 1.4 Mg/m^3. During compaction, an aluminium plate was placed on the soil surface to evenly distribute the compaction energy (i.e., hammer blows). This plate had a thin outer ring protruding from the surface to better compact the soil and hence limit root growth in the interface between soil and pipe in accordance with Mickovski et al. (2009). During soil packing, the surface of each layer was abraded to achieve a better contact between each successive layer. A 50 mm-tall pipe edge was maintained to favour irrigation and testing of saturated hydraulic conductivity (see *Saturated hydraulic conductivity* section).

The soil water retention curve (SWRC) of sieved and packed (1.4 Mg/m^3 density) soil was tested in 95-cm^3 cores (55 mm diameter and 40 mm high; Supplementary Fig. 1). A drying SWRC (Supplementary Fig. 1a) was measured for five soil cores using a ceramic suction plate (for matric suction from 1 to 50 kPa) and a pressure plate apparatus (50–1500 kPa pressure; Soilmoisture Equipment Corp, USA). A drying-wetting SWRC was also measured in a further five replicate cores on the ceramic suction plates, increasing suction up to 50 kPa and then gradually decreasing it to 1 kPa (Supplementary Fig. 1b). Water content at saturation averaged 0.35 ± 0.01 g/g. The theoretical available water content (i.e., the difference between the water content at field capacity (5 kPa matric suction) and the water content at the permanent wilting point (1500 kPa matric suction)) was 0.20 g/g. The SWRCs were fitted by the equation proposed by van Genuchten (1980):

$$w = w_r + \frac{w_S - w_r}{[1 + |\alpha\Psi|^n]^m} \quad (1)$$

where w is the soil water content (g/g), w_r is the residual soil water content at 1500 kPa (g/g), w_s is the saturated soil water content (g/g), Ψ is the soil matric suction (kPa), α, n, and m are parameters directly dependent on the shape of the curve, where $m = 1–1/n$ and $0 < m < 1$. The relation between matric suction and water content in the drying-wetting curves (Supplementary Fig. 1b) demonstrated a hysteresis loop. For instance, water content at 5 kPa matric suction was 19% smaller in the wetting path of SWRC (0.26 ± 0.00 g/g) compared to the drying path of SWRC (0.32 ± 0.00 g/g). However, the two curves come closer and overlap at their dryer ends (e.g., 50 kPa).

2.2. Selected species

Six native herbaceous species belonging to three contrasting functional types (Forbs, grasses, and legumes) were selected for testing in this study (Table 1). Species selection excluded therophytes (annual species) given their short life cycle and avoidance of unfavourable conditions. The choice of species was based on the availability of seeds, and contrasting adaptations to soil moisture as indicated by Ellenberg's indicator values (Hill, 1999), as well as laboratory germination tests. Species presenting low germination or requiring complex treatments to break seed dormancy (e.g., vernalisation) were excluded. The selected species are commonly found in European dry and wet meadows.

In April 2019, three pre-germinated seeds were sown in each vegetated soil column as a monoculture or species mix (three different species and functional types: Table 1) at the three corners of an equilateral triangle (60 mm side centered within the column). Species mixes were representative of dry and wet meadow communities on the base of Ellenberg's indicator values (CDM and CWM; Table 1). Immediately after sowing, each soil column was irrigated with 200 ml of water. All soil columns were randomly arranged in an unheated glasshouse with no additional light or heat provided. The glasshouse temperature and relative humidity were thus close to the outdoor conditions at The James Hutton Institute (Dundee, Scotland) during the entire study period (April – Sept 2019). During plant establishment (April – June), all soil columns (i.e., vegetated and control) were subjected to the same irrigation schedule ranging from 30 to 60 ml, three times per week. The amount of water per week (e.g., 90 or 180 ml) aimed to avoid any form of plant water stress or soil surface drying (i.e., water was supplied ad libitum).

2.3. Saturated hydraulic conductivity

After plant establishment (April – June 2019), the soil columns were tested for saturated hydraulic conductivity (K_s). Prior to K_s testing, soil columns were saturated in a large plastic box with the bottom covered with a mix of sand and gravel. Groups of four columns with different treatments (randomly selected) were placed in the box on the sand-gravel layer and then saturated, progressively increasing the water table by filling the box with tap water. After 24 h saturation, the columns were removed from the box and a Mariotte bottle was connected near the top of the column to apply a constant ponding head (30 mm) at the soil surface, while allowing free drainage at the column base. The rate of change in water volume in the Mariotte bottle was recorded continuously until a steady state infiltration was reached. Saturated hydraulic conductivity (K_s) of each column was then calculated using the Darcy's Law (Eq. (2)):

$$K_s = \frac{L_s}{(L_s + H)} \times \frac{Q}{S_s} \quad (2)$$

where L_s and H (m) are the sample length (i.e., column height) and the height of the water constant-head, respectively. Q (m^3/s) is the constant flow rate and S_s (m^2) is the soil surface area (i.e., soil cross-section area).

The relative surface infiltration rate between contrasting soil columns (i.e., different treatments) was also estimated, measuring the time (s) needed for the complete infiltration of a known water volume (75 ml) in a metal ring (55 mm diameter; 40 mm height) placed on the soil surface (i.e., small single-ring infiltrometer). This simple measurement was performed during contrasting soil conditions given by the antecedent soil saturation or evapotranspiration period (see next section). This method provides a rapid measurement of the soil's ability to infiltrate water after intense rain events or flash floods happening after both a wet and dry season. This method gives a relative comparison between treatments.

2.4. Evapotranspiration, matric suction and penetration resistance

After *Ks* measurements, all 45 soil columns (40 vegetated columns and 5 controls with fallow soil) were placed in a large (1 × 1 × 1 m) box on a fine layer (≈ 10 mm) of sand and gravel for saturation. All columns were saturated at the same time by filling the box to column height (≈ 0.45 m) with tap water. After 24 h, water was drained, and soil columns were randomly re-arranged in the glasshouse. Each column was then left for evapotranspiration (ET, vegetated columns) and evaporation (E, fallow columns) for 21 days (30th July – 19th Aug 2019). Water loss was monitored by weighing the columns every 2–3 days using a balance (ExplorerPro, Ohaus, Switzerland) with an accuracy of 0.1 g. The measured water loss was assumed equal to the ET in planted columns and E in fallow columns. Water loss was expressed as g of water per 100 g of dry soil. The initial and final water content of soil was estimated knowing the weight of different elements composing the columns (e.g., container PVC pipe and dry soil).

Matric suction was recorded in one soil column for each treatment using a miniature tensiometer (SWT-5, Delta-T devices, Cambridge, UK), for a total of nine monitored columns. Miniature tensiometers were horizontally installed at 0.05, 0.22 and 0.35 m below the soil surface, each through a 6.5 mm diameter hole predrilled in the pipe wall.

Maximum penetration resistance (in MPa) was measured in each soil column using a portable penetrometer (Basic Force Gauge, Mecmesin, UK; cone diameter = 2.96 mm; cone angle = 30°). To allow for the penetration tests, 3.1 mm diameter holes were drilled in the pipe wall prior to each test. Maximum soil resistance was determined by horizontally pushing the cone 35 mm into the soil in the middle of the soil column (0.22 m soil depth). Penetration resistance tests were performed immediately after saturation (i.e., matric suction close to 0 kPa) and after the evapotranspiration period (i.e., soil drying).

2.5. Soil water retention curves, porosity and wet aggregate stability

At the end of the growing season (Oct 2019), intact soil cores (50 mm diameter; 60 mm height) were sampled from the central portion of each soil column at a depth between 10 and 70 mm below the soil surface. Sampled cores were then saturated (24 h in degassed water) and tested for soil water retention properties (drying SWRCs) using a ceramic suction plate (for matric suction from 1 to 50 kPa) and a pressure plate apparatus (50–1500 kPa; Soilmoisture Equipment Corp, USA). The SWRCs were fitted by the equation proposed by van Genuchten (1980) (Eq. (1)). Soil water retention curves were used to estimate different soil

Table 1
A list of the species and communities (combinations of three species) selected for testing in this study. Their family, functional type, common name and the acronym used throughout this study are reported. The *Community* column gives the combination of three species and acronyms. Dry meadow species: *Lotus corniculatus, Festuca ovina, Daucus carota*; Wet meadow species: *Lotus pedunculatus, Deschampsia cespitosa, Geum rivale*.

Species	Family	Functional type	Common name	acronym	Community (acronym)
Lotus corniculatus	Fabacea	Legume	Birdsfoot Trefoil	L-LC	
Festuca ovina	Poacea	Grass	Sheep's Fescue	G-FO	Dry meadow (CDM)
Daucus carota	Apiacea	Forb	Wild Carrot	F-DC	
Lotus pedunculatus	Fabacea	Legume	Greater Birdfoot Trefoil	L-LP	
Deschampsia cespitosa	Poacea	Grass	Tufted Hair-grass	G-DC	Wet meadow (CWM)
Geum rivale	Rosacea	Forb	Water avens	F-GR	

parameters including water content at field capacity (water content (*w*) at 5 kPa), air content at field capacity (i.e., difference between volumetric *w* at saturation and *w* at field capacity) and plant available water (i.e., difference between *w* at 5 kPa and *w* at 1500 kPa).

During each SWRC testing (i.e., progressive soil drying), soil penetration resistance (in MPa) was determined on each soil core equilibrated at 5, 20 and 300 kPa matric suction. Penetration resistance was determined using a universal testing frame (Instron 5966, Norwood, MA, USA) fitted with a 50 N load cell (± 2 mN accuracy). In each core a small cone probe (0.95 mm; 30° cone angle) was penetrated to 15 mm depth from the soil surface with a rate equal to 4 mm/min. Penetration resistance between 4.5- and 9.8-mm depth was averaged. Note that the average penetration resistance was always smaller (e.g. - 30 or 40%) than the maximum penetration resistance recorded in the manually pushed cone tests. The cone diameter and penetration depth were chosen according to the core size to avoid any boundary effect (Misra and Li, 1996).

Pore volume for different pore diameter classes, defined in Greenland (1981) (from >300 to <0.2 μm), was estimated from SWRC data. The effective pore diameter (*d*) corresponding to the matric suction (Ψ) tested in the SWRCs was calculated using Jurin's formula (Eq. (3)).

$$d = 4 \times \frac{\sigma}{\Psi} \tag{3}$$

where the surface tension is $\sigma = 7.29 \times 10^{-2}$ N m^{-1} and Ψ is in Pa. For instance, the effective diameter of a pore corresponding to 1500 kPa is 0.2 μm. Volume of pores in each diameter class was estimated by changes in volumetric water content in the SWRCs.

Samples of bulk soil were also collected at 10–100 mm below the soil surface and air-dried in the laboratory to test the wet stable aggregates (*WSA*) in each soil column. A 5.3 g subsample of air-dried soil, passing an 8-mm sieve and being retained on a 2-mm sieve was used to test *WSA* in a wet sieving apparatus (Eijelkamp Soil & Water, Netherlands). In the wet sieving apparatus, 2-mm-mesh sieves filled with the air-died soil (5.3 g) were mechanically moved up and downward (up-down strokes = 1.3 cm) in a can filled with distilled water for 3 min ± 5 s (34 times/min up-down strokes). Unstable aggregates fell apart and passed through the 2 mm sieve into the water-filled can under the sieve. Subsequently, the cans with soil from unstable aggregates were removed and replaced by new water filled cans. All stable aggregates retained on the sieve mesh were fully destroyed and soil from the stable aggregates was collected in the water can. Note that any gravel particles and plant roots remained on the sieve and only the soil from the aggregates passed into the water cans. After drying, the two sets of cans with the soil from unstable and stable aggregates, aggregate stability of *WSA* was calculated using the weight of both stable (*SA*) and unstable aggregates (*UA*) by Eq. (4).

$$WSA = \frac{SA}{(SA + UA)} \tag{4}$$

2.6. Above- and below-ground plant characteristics

After the monitoring of evapotranspiration (August 2019), aboveground biomass was harvested in all vegetated columns and quantified through oven drying at 70 °C until a constant weight was obtained. Following soil sampling for aggregate stability and water retention testing, rooted soil columns were removed from pipes and sectioned into three cores corresponding to three depth ranges: 0.00–0.13 m, 0.13–0.26 m, 0.26–0.40 m. Roots in each section were washed from the soil in gently running tap water on a set of sieves with a range of sieve sizes from 2.0 to 0.5 mm mesh. Sampled roots were stored at 5 °C in 40% ethanol solution before root scanning and biomass quantification (oven-drying). Roots at the three soil depth ranges were imaged on a flatbed scanner and analysed using WinRhizo software (Regent Instruments Inc.) to determine total root length and root length per diameter class (diameter classes: 0.1 mm interval width; roots from <0.1 to 10 mm). In the case of large root systems, representative subsamples (= 10 to 95% of root biomass) were scanned. Measured length and biomass (oven-dried at 70 °C) of scanned subsamples were then used to obtain the specific root length (SRL, root length by mass; m/g). The total root length in each section was then estimated by multiplying the dry root biomass by the SRL. Thicker roots of *Daucus carota* were scanned and analysed separately. Root volume per each diameter class was also estimated using WinRhizo image analysis.

2.7. Statistical analysis

Statistical analysis was performed using GenStat 17th Edition (VSN International), RStudio (R-version 3.6.2; R Foundation for Statistical Computing) and SigmaPlot13 (Systat Software Inc). Significant differences were assessed with one way-ANOVA, followed by post hoc Tukey's test. Non-normal data were log or square root transformed before ANOVA tests. Results were considered statistically significant when *p*-value ≤0.05. Principal-component analysis was conducted to examine the relationships between traits and soil parameters. The variability in the averaged result is presented as ± standard error of mean. Details (e.g., *p*-values, log-transformation) of statistical analyses for each dataset are provided in the text and in figure captions.

3. Results

Plant growth in soil columns increased saturated hydraulic conductivity (K_s). On average K_s of vegetated soil ($3.2e^{-5} \pm 2.0e^{-6}$ m/s) was four times larger than that of control fallow soil ($6.9e^{-6} \pm 1.4e^{-6}$ m/s; Fig. 1a). However, tested species differed in their effect on K_s, ranging from $9.9e^{-6} \pm 1.3e^{-6}$ m/s of *Festuca ovina* (Grass) to $4.1e^{-5} \pm 3.7e^{-6}$ of *Lotus pedunculatus* (Legume; Fig. 1a). In particular, *F. ovina* did not significantly affect K_s when compared to the control fallow soil. In contrast, both legumes (*Lotus* spp.) differed significantly from the control soil and the two tested grasses but did not significantly differ between each other. Indeed, no significant difference was observed between species from the same plant functional type as well as the two simple species communities (CDM and CWM in Fig. 1a).

The results from the single-ring infiltrometer further highlighted the large differences between treatments in terms of soil ability to absorb water when wet (i.e., immediately after saturation) and after a drying period (i.e., after ET; Fig. 1b). The soil surface highlighted a faster water absorption when dried by ET. Surface infiltration was significantly greater in the vegetated soil than the control soil in both wet and dry conditions (black and grey bars in Fig. 1b), with the soil vegetated with *F. ovina* being the only exception (i.e., no different from control). For example, the infiltration in the vegetated soil was up to six- (0.11 mm/s in CWM) and seven-times (0.41 mm/s in L-LC) greater than the values of control soil after saturation and ET period, respectively. The wet meadow community (CWM) showed greater water infiltration when compared with the dry meadow community (CDM), consistently in both the K_s measurements and single-ring infiltration test at saturation (Fig. 1).

Total water loss during the monitoring period was always larger in vegetated soil columns (water loss >29 g H_2O per 100 g of dry soil) when compared with control columns (water loss = 5.5 ± 0.1 g H_2O per 100 g of dry soil; Fig. 2). However, a large species effect existed, with an average water loss per day ranging from 1.1 ± 0.1 to 2.6 ± 0.1 g H_2O per 100 g of dry soil in *F. ovina* and *Lotus corniculatus* respectively. In particular, *L. corniculatus* highlighted an initial fast water loss (up to 4.0 ± 0.3 g H_2O per 100 g of soil per day), which then slowed down with the progress of the drying period (e.g., after 10 days) until reaching a daily water loss of 1.4 ± 0.0 g H_2O per 100 dry soil (Fig. 2a). The difference in water loss between fallow (i.e., evaporation) and vegetated columns (i.e., ET) provided the degree of plant contribution to water removal from soil by transpiration. The estimated transpiration represented on average between 58 ± 1% (in *F. ovina*) and 82 ± 1% (in *L. corniculatus*)

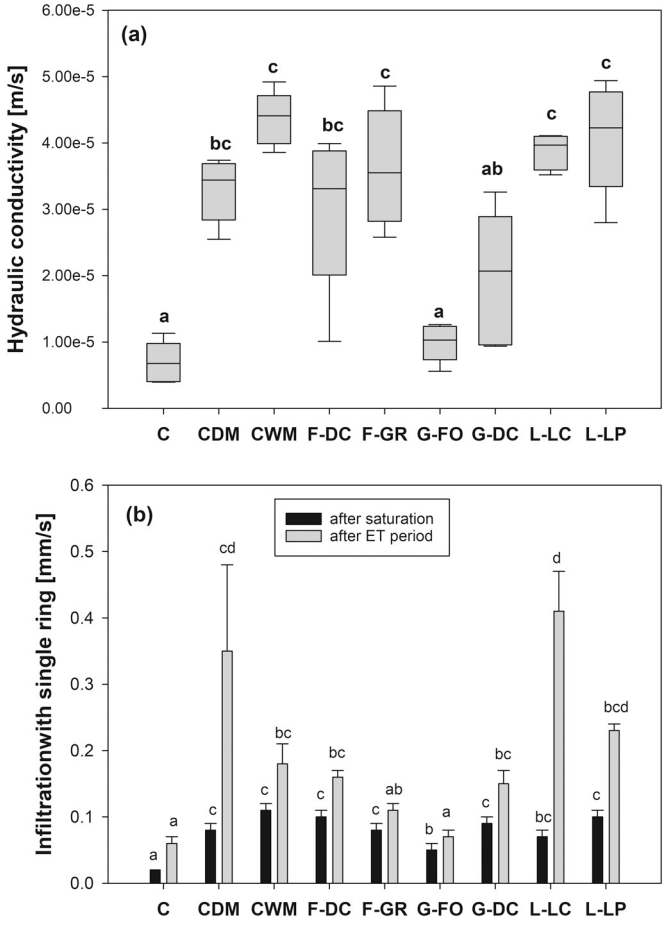

Fig. 1. **(a)** Saturated hydraulic conductivity of control (C, fallow soil) and vegetated soil columns with contrasting species. The bottom and top of boxes represent the 25th and 75th percentile, while the line within the box marks the median ($n = 5$). Whiskers (error bars) above and below the box indicate the 90th and 10th percentiles. (**b**) Infiltration measured using the simple single-ring test after saturation (black vertical bars) and after 21 days of evapotranspiration (ET; grey vertical bars). Means are reported ± standard error of mean (n = 5). Different letters in a and b graphs indicate a statistically significant difference between treatments, as tested using one-way ANOVA (*p-value* < 0.001) followed by post hoc Tukey's test. Acronyms: C (Control); CDM (Dry meadow community); CWM (Wet meadow community); F-DC (*Daucus carota*); F-GR (*Geum rivale*); G-FO (*Festuca ovina*); G-DC (*Deschampsia cespitosa*); L-LC (*Lotus corniculatus*) and L-LP (*Lotus pedunculatus*).

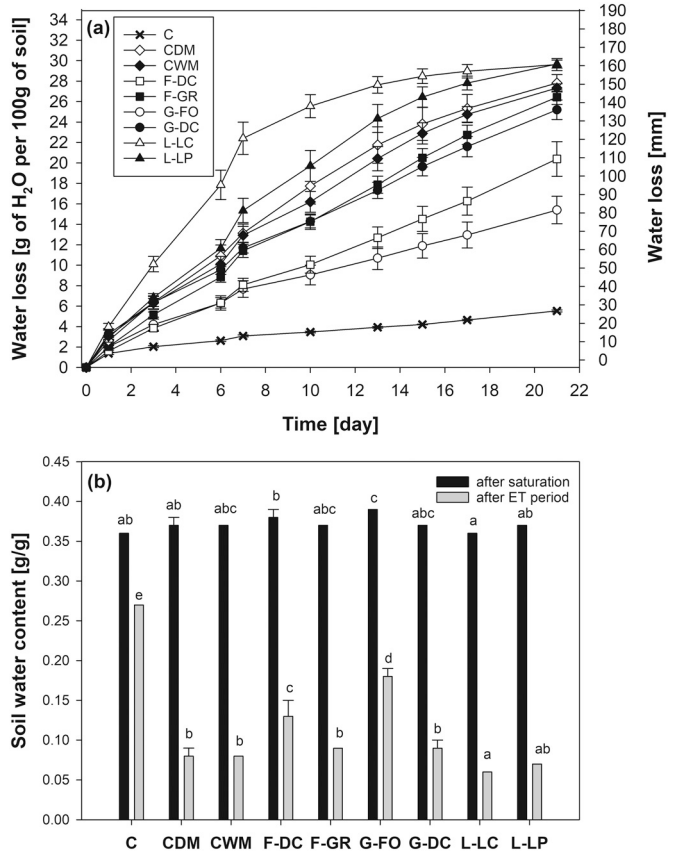

Fig. 2. (**a**) Water loss from fallow (control) and vegetated soil columns during the 21-day monitoring period (30th July – 19th Aug 2019) after soil saturation (day 0). On the left y-axis, water loss is normalised by dry soil weight, while on the right y-axis water loss is presented as water depth in mm (water loss (l) per soil surface (m^2)). Means are reported ± standard error of mean ($n = 4$). (**b**) Soil water content (g of water per g of dry soil) of fallow (control) and vegetated soil columns immediately after saturation (black vertical bars) and after evapotranspiration monitoring (grey vertical bars). Means are reported ± standard error of mean ($n = 5$). Different letters in graphs a and b indicate a statistically significant difference between treatments, as tested using one-way ANOVA (*p-value* < 0.001) followed by post hoc Tukey's test. Acronyms: C (Control); CDM (Dry meadow community), CWM (Wet meadow community); F-DC (*Daucus carota*); F-GR (*Geum rivale*); G-DC (*Deschampsia cespitosa*); G-FO (*Festuca ovina*); L-LC (*Lotus corniculatus*) and L-LP (*Lotus pedunculatus*).

of daily water loss (i.e., ET) from vegetated columns.

The differences in water loss between treatments (Fig. 2a) translated to significant differences in soil water content (Fig. 2b). While water content in fallow soil remained close to field capacity during the entire monitoring period, water content of vegetated soil dropped below the value of permanent wilting point in most of the vegetated columns (0.11 g/g see SWRC in Supplementary Fig. 1a).

Matric suction induced by soil drying largely differed between treatments, soil depth and time (Fig. 3). In fallow soil, matric suction did not exceed 11 kPa down the entire soil profile during the monitoring period. In the shallow soil layer (Fig. 3a), all vegetated soil columns developed large matric suction values (> 70 kPa) except for the soil vegetated with *D. carota* (≤ 20 kPa). However, large differences between vegetated treatments were recorded in terms of the time required to reach these large suction values. For instance, while soil vegetated with *Lotus* spp. developed large matric suction values in only one week, soil columns vegetated with grasses took almost double the time to reach the same matric suction values (80 kPa). The time required to induce large matric suction values increased with increasing depth down the soil profile. In the middle and bottom layers of the soil columns (0.22 and 0.35 m; Fig. 3bc), both *D. carota* and *F. ovina* were unable to induce large matric suction values despite the long drying period. In contrast, soil vegetated with *Lotus* spp. developed large matric suction values down the entire soil profile.

Soil strength (measured as penetration resistance) in the middle section of the soil columns largely varied in response to soil moisture content and plant drying ability (Figs. 2, 3 and 4). Although all treatments (i.e., fallow and vegetated columns) showed a significant strength increase with drying, strength gain varied largely between different treatments (Fig. 4). While in the fallow soil, evaporation resulted in a 1.5-times stronger soil compared to the value recorded after saturation, ET in vegetated soil induced a strength gain up to 12-times (in *L. corniculatus*) the value measured in saturated soil. Tested species significantly differed in their ability to induce strength gain after the ET period. While the soil vegetated with *L. corniculatus* was 25-times stronger than the control fallow soil (see grey bars in Fig. 4), soil vegetated with *F. ovina* was not significantly stronger than the control soil. Although, after saturation, the strength differences between control and vegetated columns were smaller compared to the values observed

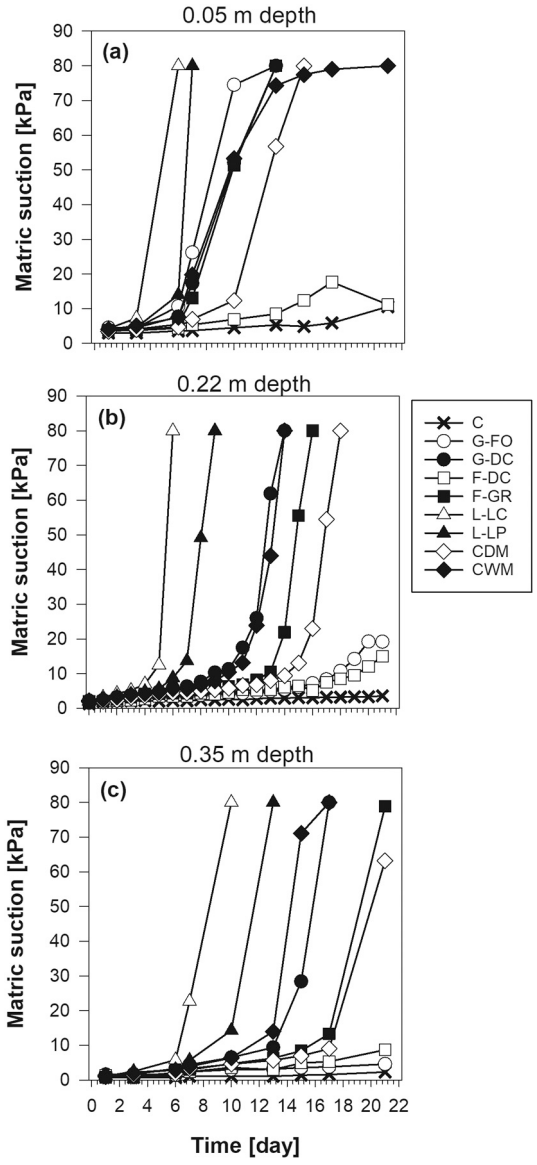

Fig. 3. Matric suction recorded in control and vegetated soil columns at 0.05 (**a**), 0.22 (**b**) and 0.35 (**c**) m depths during progressive soil drying after soil saturation (30th July – 19th Aug 2019). Acronyms: C (Control); CDM (Dry meadow community), CWM (Wet meadow community); F-DC (*Daucus carota*); F-GR (*Geum rivale*); G-DC (*Deschampsia cespitosa*); G-FO (*Festuca ovina*); L-LC (*Lotus corniculatus*) and L-LP (*Lotus pedunculatus*).

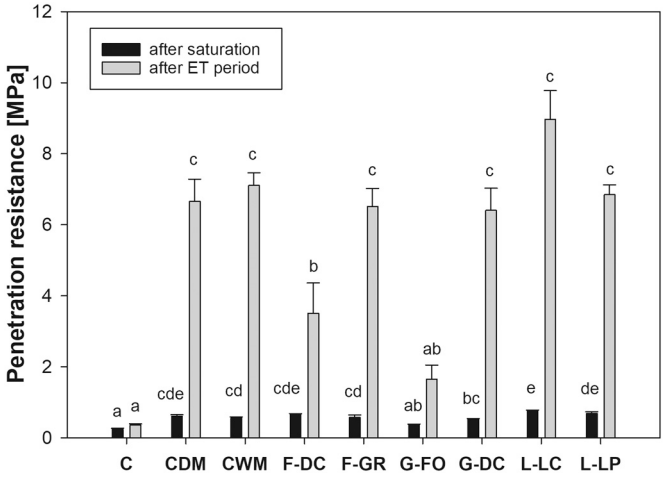

Fig. 4. Penetration resistance (i.e., soil strength) measured in the middle section (0.22 m depth) of fallow and vegetated soil columns after saturation (black vertical bars) and after 21 days of evapotranspiration (ET; grey vertical bars). Tests were performed horizontally penetrating the soil column with 2.96 mm cone diameter and recording the maximum value of resistance. Means are reported ± standard error of mean ($n = 5$). Different letters indicate a statistically significant difference between treatments, as tested using one-way ANOVA (*p-value* < 0.001) followed by post hoc Tukey's test. Acronyms: C (Control); CDM (Dry meadow community), CWM (Wet meadow community); F-DC (*Daucus carota*); F-GR (*Geum rivale*); G-DC (*Deschampsia cespitosa*); G-FO (*Festuca ovina*); L-LC (*Lotus corniculatus*) and L-LP (*Lotus pedunculatus*).

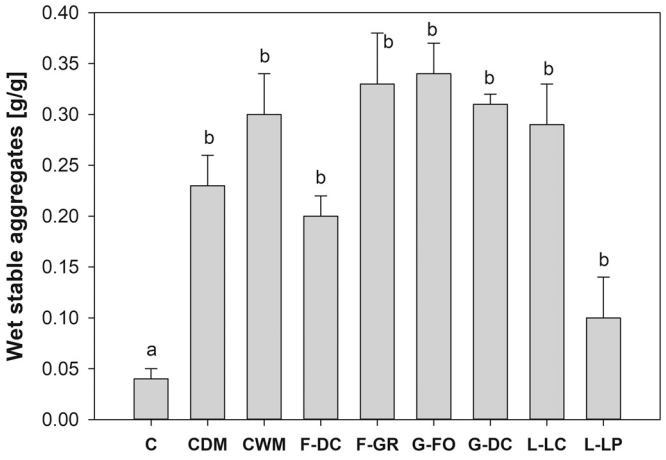

Fig. 5. Wet stable aggregates measured in soil sampled from fallow and vegetated soil columns. Means are reported ± standard error of mean ($n = 5$). Letters indicate a statistically significant difference between treatments, as tested using one-way ANOVA (*p-value* < 0.001) followed by post hoc Tukey's test. Acronyms: C (Control); CDM (Dry meadow community), CWM (Wet meadow community); F-DC (*Daucus carota*); F-GR (*Geum rivale*); G-DC (*Deschampsia cespitosa*); G-FO (*Festuca ovina*); L-LC (*Lotus corniculatus*) and L-LP (*Lotus pedunculatus*).

after ET, it should be noted that most of the vegetated columns were significantly stronger (2-times) than the control soil (see black bars in Fig. 4).

The measurement of wet stable aggregates (*WSA*) highlighted significant differences between control fallow soil and vegetated soil in the tested columns (Fig. 5). While only 4% of the aggregates from the fallow soil did not dissolve in water and wash out (i.e., 96% of aggregates destroyed by water), in the vegetated treatments *WSA* represented between 10 and 32% of aggregates. Therefore, in the vegetated treatments up to one-third of soil was able to resist the extreme weathering and maintain its structure.

Fig. 6a shows the soil water retention curves measured in the tested treatments (data points in Supplementary Fig. 2; fitting parameters in Supplementary Table 1). At saturation, soil water content ranged between 0.34 and 0.36 g/g. Significant differences in water holding capacity were observed at field capacity (i.e., soil equilibrated at 5 kPa; Fig. 6b). Indeed, water content at field capacity highlighted significantly smaller values in control soil and soil vegetated with both grass species (*Festuca ovina* and *Deschampsia cespitosa*) compared to soil vegetated with the species mix (i.e., dry and wet meadow communities). Similarly, these treatments (control soil and grasses) highlighted significantly larger air content at field capacity compared with the other vegetated treatments (Fig. 6c). On the contrary, plant communities (CDM and CWM) and *Daucus carota* induced a significant drop of soil air content at field capacity (Fig. 6c). The effects of contrasting plant functional types were further highlighted by the values of plant available water estimated from SWRCs (Fig. 6d). Indeed, soil vegetated with plants

belonging to the same functional type exhibited consistent values of estimated available water.

Data of soil pore size (Fig. 7), estimated from the SWRCs, shows interesting effects of contrasting species on different pore diameter classes and hence soil functions (Greenland, 1981). Macro-porosity, responsible for soil aeration (> 300 μm), highlighted a significant drop (≈ 60%) in the soil vegetated with the wet meadow community, *Daucus carota* and *Lotus pedunculatus*, when compared with the control soil, where macropores accounted for 4% of total core volume. Pores responsible for water drainage in soil (300–30 μm) showed significant differences between the vegetated treatments, where both legumes exhibited significantly larger volumes of drainage pores compared to both grasses and the forb *D. carota*. Noteworthy is the consistent effect of species belonging to the same family (i.e., functional type). The pore diameter class ranging between 300 and 30 μm was the most represented in the cores sampled from vegetated columns. For example, these pores represented on average 23% of total pore volume in the dry meadow treatment. While pores in the diameter range 300–30 μm generally increased in vegetated cores (compared with control), micropores (< 0.2 μm) showed the opposite trend. When the diameter classes "300 – 30 μm" and "< 0.2 μm" are considered, grasses and legumes highlighted opposite trends of pore volume changes.

Soil penetration resistance measured during SWRC testing highlighted a large strength increase with soil drying (i.e., during SWRC; Fig. 8). In particular, the greater strength gains with drying (e.g., from 5 to 20 kPa) were recorded in the fallow control soil and the soil vegetated with the two grass species (up to 4.2-times increase). Similarly, a matric suction increase from 5 to 300 kPa confirms the larger strength gain in control and grass-vegetated soils. While the control soil and soil vegetated with grasses were between 14- and 16-times stronger at 300 kPa (compared to 5 kPa); in the soil vegetated with the other species and plant communities, the increase did not exceed 10-times the value at 5 kPa. Penetration resistance in *D. carota* and *D. cespitosa* treatments differed significantly when the soil was equilibrated to 5 kPa matric suction, where *D. carota* soil exhibited the greatest penetration resistance (0.48 ± 0.08 MPa). In contrast, the grass *D. cespitosa* showed the weakest soil (0.23 ± 0.02 MPa). Despite the large variability in penetration resistance, the soil vegetated with the same plant types (e.g., same family) highlighted consistent strength. When soil cores were equilibrated at 20 and 300 kPa suction, no statistically significant difference was observed.

Five months after sowing, all plants in the soil columns showed proper development and growth (i.e., no species highlighted clear signs of stress or poor growth). As expected, above-ground biomass largely differed between the tested species, with the smallest and largest above-ground biomass recorded in *D. carota* (4.39 ± 0.21 g) and *Lotus corniculatus* (11.69 ± 0.24 g), respectively (Fig. 9a). In the plant communities (CDM and CWM), the relative contribution to above-ground biomass varied largely between species (e.g., in CDM: 48 ± 13% *D. carota*; 49 ± 12%; *L. corniculatus*; 3 ± 1% *F. ovina*).

Above-ground differences between plants did not always translate to similar below-ground differences (Fig. 9ab). Generally, most of the root biomass was found in the shallow soil layer (0.00–0.13 m). In the deeper soil layers root biomass highlighted a sharp decrease (Fig. 9b). *D. cespitosa* soil columns represented an exception to this general trend having the largest root biomass in the deepest soil layer. Indeed, *D. cespitosa* roots reached the bottom of the column and grew largely in the deeper soil layer.

Root length measured down the soil profile varied significantly between treatments. Interestingly, the largest and smallest root length values were measured in the deep soil layer (0.26–0.40 m) of the columns vegetated with the two grasses (G-FO = 5.11 ± 3.64 m; G-DC = 370.07 ± 65.89 m; Fig. 9c). In soil columns vegetated with grasses (i.e., fibrous roots), root length down the soil profile highlighted similar trends to biomass values (Fig. 9 b, c). On the contrary, in forb and legume species large biomass values did not translate into large root length values. For example, *D. carota* exhibited large biomass and small root length values in the shallow soil (0.00–0.13 m). Moreover, while biomass generally decreased with soil depth, root length increased with soil depth in different treatments (e.g., CWM; L-LC; L-LP in Fig. 9c). The increase in root length down the soil profile can be explained by a greater specific root length (SRL) in the deeper soil layers (Fig. 9d). Large differences in SRL between species and soil layers (i.e., depths) were the results of biomass allocation in different root diameter classes, as highlighted by root length and volume per diameter classes in Supplementary Figs. 3 and 4. In all treatments, most of the root length was represented by fine roots, with diameter thinner than 0.5 mm (Supplementary Fig. 3). Thicker roots (e.g., > 3 mm) represented less than 0.1% of root length. On the contrary, root volume per diameter class highlighted large differences between treatments. For instance, in the shallow soil of *D. carota* and the dry meadow community columns, most of the root volume was represented by thick roots (> 3 mm) (Supplementary Fig. 4).

The PCA biplot in Fig. 10 highlights the relation between the main investigated variables (i.e., plant traits and soil parameters). The first two components of the PCA account for 56% of variation. The first PCA axis (Dim 1) is strongly correlated with soil hydrological parameters, such as plant available water (PAW, Pearson's $r = 0.90$), water content at field capacity (FC, Pearson's $r = 0.78$) and saturated hydraulic conductivity (Ks, Pearson's $r = 0.76$), but negatively correlated with specific root length (SRL, Pearson's $r = -0.85$) and volume of pores with diameter thinner than 0.2 μm. The second PCA axis (Dim 2) is positively correlated with shoot biomass (S.BM, Pearson's $r = 0.82$), air content at field capacity (AC, Pearson's $r = 0.74$) and daily evapotranspiration (WL_d, Pearson's $r = 0.55$). Specific root length was negatively correlated with both hydraulic conductivity and plant available water (vectors in opposite directions). Penetration resistance showed a positive relation with daily evapotranspiration (small angle between vectors between PR_ET and WL_d). Significant and notable correlations highlighted by the PCA biplot (WL_d vs PR_ET; SRL vs Ks; SRL vs PAW) are shown in greater detail (scatter plots) in Fig. 11.

4. Discussion

This study highlighted multiple soil-plant interactions that may influence the performance of vegetated earth barrier systems in reducing flood risk. For instance, hydraulic conductivity (K_s) of vegetated soil was generally larger than that of control fallow soil. However, the tested species differed in their effect. The water infiltrated and stored in the soil was efficiently removed by plant transpiration, recharging the storage capacity of soil. In the vegetated soil, daily evapotranspiration resulted in up to five times greater water loss compared to the fallow soil. During a single growing season (April – August), profound changes on soil structure were observed with a significant increase in aggregate stability and alteration of water retention properties. The following sections discuss the effects of the different species and communities on soil hydro-mechanical properties in turn.

4.1. Effect of plants on water infiltration

Most of the tested species significantly increased the saturated hydraulic conductivity (K_s) of soil. Increased water infiltration in the presence of vegetation has been reported for both woody and herbaceous plants (Archer et al., 2015; Ghestem et al., 2011; Leung et al., 2018; Ng et al., 2020). The increases in infiltration and hydraulic conductivity have been explained with the preferential flow of water along root channels formed around live, decaying or dead roots (Ghestem et al., 2011; Ni et al., 2019), as well as along desiccation cracks upon transpiration induced drying (Song et al., 2017). In particular, Archer et al. (2013) reported a significant increase in soil hydraulic conductivity in broad-leaf woodlands compared with degraded grasslands. Indeed, it is now commonly recognised that trees can enhance water

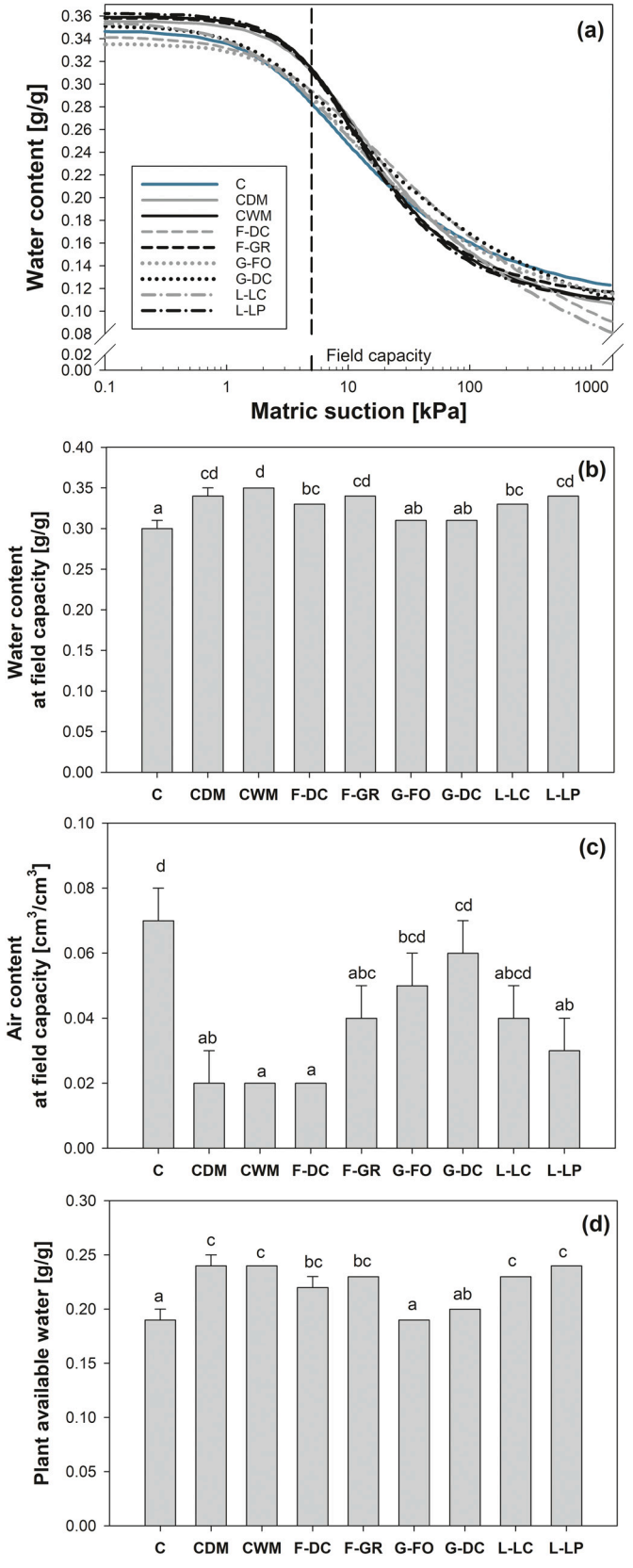

Fig. 6. (**a**) Soil water retention curves obtained using the van Genuchten (1980) model to fit water content data measured in cores equilibrated to different pressure values (on ceramic suction plate and pressure chambers). Data-points and model parameters are presented in Suppl.Fig. 2 (i.e., scatter plot) and Suppl. Table 1. Vertical dashed line indicated field capacity (i.e., 5 kPa matric suction). RETC software (PC-progress) was used to fit the water retention data; (**b**) Water content at field capacity; (**c**) air content at field capacity; (**d**) plant available water estimated from water retention curves of soil cores sampled from fallow and vegetated soil columns. Means are reported ± standard error of mean ($n = 5$). Different letters indicate a statistically significant difference between treatments, as tested using one-way ANOVA (*p-value* < 0.001) followed by post hoc Tukey's test. Acronyms: C (Control); CDM (Dry meadow community), CWM (Wet meadow community); F-DC (*Daucus carota*); F-GR (*Geum rivale*); G-DC (*Deschampsia cespitosa*); G-FO (*Festuca ovina*); L-LC (*Lotus corniculatus*) and L-LP (*Lotus pedunculatus*).

infiltration and hence decrease runoff during storm events (Archer et al., 2013; Ghestem et al., 2011; Greenwood and Buttle, 2014). In contrast, more contradictory results have been reported for herbaceous plants. For instance, Gish and Jury (1983) and Jotisankasa and Sirirattanachat (2017) observed a decrease (compared with fallow soil) in hydraulic conductivity in soil vegetated with *Triticum aestivum* and *Chrysopogon zizanioides*, respectively. A similar observation has also been reported in a field study of grass and woody species (Leung et al., 2015a). These decreases in hydraulic conductivity were explained with root clogging of soil pores, and consequent blockage of water flow paths.

Although our results and the literature show a general increase in K_s in vegetated soil, it is an oversimplification not to consider the species effect, in particular for herbaceous species where extremely contrasting root systems exist in terms of depth, morphology and turnover dynamics (Pagès, 2011). Our results (Figs. 1) highlighted the significance of the species-effect on infiltration and hydraulic conductivity. The lack of a difference in K_s between fallow soil and soil vegetated with *F. ovina* can be explained by the fibrous root system of *F. ovina*, where most of the root length and volume fell in diameter classes smaller than 2 mm (Supplementary Figs. 3 and 4). Indeed, K_s was negatively correlated with specific root length (SRL) (Fig. 11a). This observation can be explained by the small root-soil interface of fine roots along which preferential flow may occur (Ghestem et al., 2011), as well as the limited soil deformation during root penetration. Moreover, the dense and shallow root system of *F. ovina* (Fig. 9) might have resulted in a root mat which was able to prevent the formation of cracks, as well as clog macropores, in agreement with a study by Song et al. (2017) on the hydraulic properties and cracking of soil vegetated with *Cynodon dactylon* (grass). In contrast, species with thick roots (e.g., *D. carota*; Supplementary Fig. 4g–i) and high transpiration (*Lotus* spp.; Fig. 2a) may have induced the formation of soil cracks due to radial root growth and desiccation cracks upon fast soil drying. Cracks were observed on the soil surface of some columns vegetated with *D. carota* and *Lotus* spp. Previous studies associated large changes in soil hydraulic properties with the presence of coarse roots (diameter > 2 mm) (Archer et al., 2013) and desiccation cracks (Song et al., 2017). Furthermore, a deep root system could have resulted in a continuum of preferential flow paths along the entire soil volume, while the effect of shallow root systems (e.g., *F. ovina*; Fig. 9b) may have been limited to the topsoil layer. The number and size of cracks, as well as connection and tortuosity of root channels might have caused a large heterogeneity in soil and the notable variability of hydraulic conductivity in vegetated soil (Fig. 1).

In this study, the K_s was tested after plant establishment (i.e., young plants) and it is likely that the hydraulic conductivity of vegetated soil will keep changing as roots grow and decay. For instance, a linear increase in K_s during plant growth (i.e., time since establishment) was observed in soil vegetated with *Salix viminalis* (shrub) and *Lolium perenne* x *Festuca pratensis* hybrid (Festulolium grass) (Leung et al., 2018). On the other hand, Vergani and Graf (2016) found that K_s of soil vegetated with *Alnus incana* increased until a threshold value of root length density (0.1

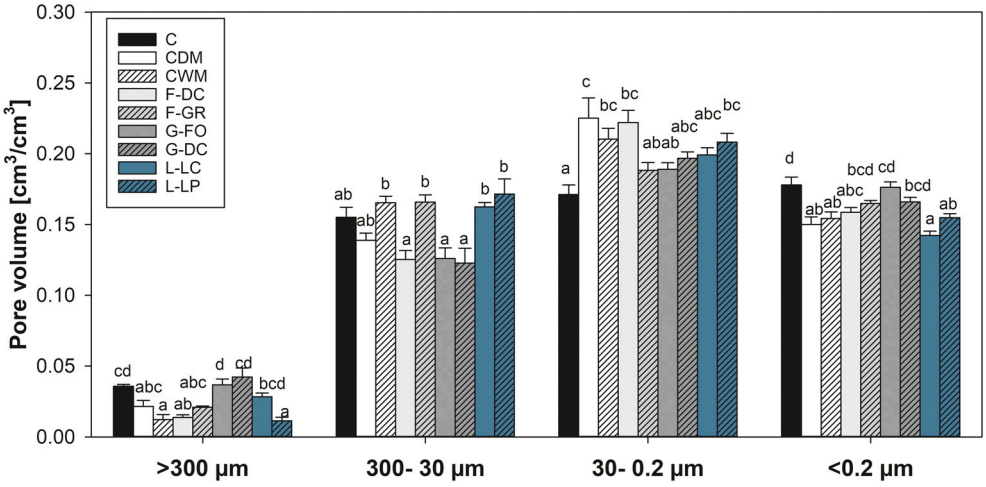

Fig. 7. Pore volume per total core volume for different diameter classes associated with different aeration and water retention functions: (i) aeration pores >300 µm; (ii) drainage pores 300–30 µm; (iii) slow drainage and retention pores 30–0.2 µm; (iv) < 0.2 µm pores retaining non-available water for plants. Total volume of soil core was equal to 118 cm^3. Means are reported ± standard error of mean (n = 5). Different letters indicate a statistically significant difference between treatments in terms of pore volume within diameter classes (e.g., > 300 µm), as tested using one-way ANOVA (p-value < 0.001) followed by post hoc Tukey's test. Acronyms: C (Control); CDM (Dry meadow community), CWM (Wet meadow community); F-DC (*Daucus carota*); F-GR (*Geum rivale*); G-DC (*Deschampsia cespitosa*); G-FO (*Festuca ovina*); L-LC (*Lotus corniculatus*) and L-LP (*Lotus pedunculatus*).

cm/cm^3), after which K_s decreased.

It remains difficult to compare the different studies on K_s changes in vegetated soil. While field studies operate in a complex system, resulting from long-term processes such as organic matter accumulation (e.g., 4000-year-old Caledonian forest in Archer et al. (2015)), studies in controlled environments have the advantage to reduce variability and hence highlight mechanistic processes (e.g., species effect). However, laboratory and glasshouse studies have the disadvantage of introducing artificial boundary conditions associated with the use of soil cores, pots or soil columns (Vergani and Graf, 2016). Indeed, water flow between soil and container wall may differ with respect to the water flow in soil matrix and root channels. Moreover, the container diameter may indirectly influence water flow along root channels affecting the development of the root system. we can generally expect small root biomass, steeper root angles and deeper roots with the narrowing of the container diameter (Poorter et al., 2012). Therefore, it should be highlighted that our experiments were designed to make relative comparison between different treatments (e.g., species) under the same boundary conditions.

The single-ring infiltration test further highlighted and confirmed the large differences between treatments in terms of soil hydraulic properties. In particular, K_s measurements and single-ring tests provided consistent treatment (e.g., species) ranking in terms of water infiltration into the soil (Fig. 1a, b). The PCA showed an association between the two variables (Fig. 10). Immediately after saturation, the fastest infiltration values were recorded in the soil vegetated with the wet meadow community and with *L. pedunculatus* (CWM and L-LP in Fig. 1b), consistent with the K_s measurements (Fig. 1a). As expected, infiltration after saturation was mainly driven by the K_s of the soil. In contrast, infiltration after the evapotranspiration period (i.e., unsaturated conditions) may have been influenced by different factors such as soil water content, matric suction and large desiccation cracks. The water content and matric suction after ET monitoring varied largely between treatments (Figs. 2 and 3) as a result of different ET rates (Fig. 2). Therefore, soil moisture conditions during the infiltration test were not consistent between treatments and the data should be interpreted as the relative difference in the light of information on ET and soil water status (Figs. 2 and 3). For instance, the large infiltration difference between the dry and wet conditions in the dry meadow community (CDM in Fig. 1 b) might also be driven by large ET and matric suction induced by *L. corniculatus* (Figs. 2 and 3). This condition can represent the response of soils with contrasting vegetation covers to dry periods followed by intense precipitations, condition that will become common with the intensifying of climate change (IPCC, 2013; Rummukainen, 2012).

Although single-ring infiltration can generally provide only a relative measurement between treatments, it offers a validation of K_s measurements performed with the more accurate constant-head method (Mariotte bottle). In particular, it should be noted that the single ring setting has the advantage of not being affected by the container boundaries, because the test was performed on a small soil area at the centre of the soil surface (i.e., far from the pipe wall). However, test conditions, scale effect and soil heterogeneity can make measurements made by the constant-head method and single-ring not directly comparable in terms of absolute data.

4.2. Water removal by plants

Monitoring of water loss from soil columns clearly highlights the major role of plants in removing water. The estimated transpiration represented on average between 58 ± 1% (in *F. ovina*) and 82 ± 1% (in *L. corniculatus*) of daily water loss (i.e., evapotranspiration) from vegetated columns. This is consistent with the estimated contribution of transpiration (about 57%) to global terrestrial evapotranspiration (Wei et al., 2017). The tested herbaceous species were able to remove large amounts of water despite the relatively small biomass. For instance, the total mass of transpired water by *L. corniculatus* during the 21 days period (Fig. 2) was about 90-times its aboveground biomass (11.69 ± 0.24 g). Indeed, in general more than 90% of adsorbed water by plants is lost by transpiration and only 1% and 5% are retained in biomass and tissue expansion, respectively (Lambers et al., 2008). Such inefficient use of water by plants, resulting from the water/carbon dioxide gradients between atmosphere and leaf mesophyll, becomes a fundamental feature when plants are functional components of any bioretention system. After heavy precipitation, the soil can reach saturation and no more water can be stored. Part of the water stored during the rain event is lost by drainage immediately after the rain event. However, drainage stops when soil reaches field capacity (generally between 2 and 8 kPa matric suction). Evaporation, even under optimal conditions (e.g., high vapor pressure deficit), can only dry the soil surface (Figs. 2 and 3), because the drop in unsaturated hydraulic conductivity limits further water loss from depths. In contrast, the vegetation canopy expands and connects the evaporative surface (e.g., leaves) well beyond the soil surface exposed to the atmosphere. Water is extracted at least as deep as the roots can penetrate (Figs. 3 and 9b, c). Indeed, while the water content of fallow soil remained close to field capacity (0.27 g/g) despite 21 days of evaporation (representing a dry period), during the same period the water content in the vegetated soil dropped beyond the permanent wilting point (0.06 g/g in *L. corniculatus* vegetated soil). The regulation ability of transpiration by stomatal conductivity, was shown by the slowing down of the rate of water loss in *L. corniculatus* columns with the progress of drying (Fig. 2a). Indeed, in addition to the ability to

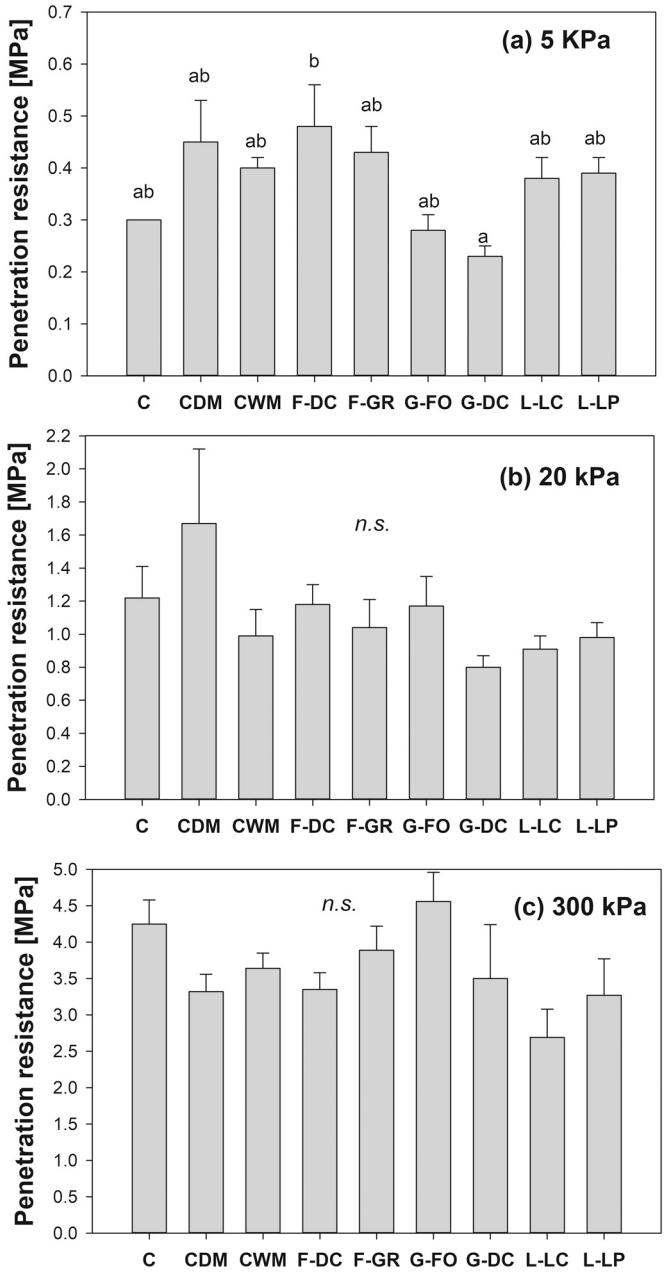

Fig. 8. Penetration resistance measured in soil cores tested for water retention at (**a**) 5 kPa, (**b**) 20 kPa and (**c**) 300 kPa matric suction. Tests were performed vertically penetrating the soil core with 0.95 mm cone diameter. Means are reported ± standard error of mean (n = 5). Different letters indicate a statistically significant difference between treatments, as tested using one-way ANOVA (p-value <0.001) followed by post hoc Tukey's test. *n.s.* indicates a lack of significant difference between treatments (p-value >0.05). Note that y-axis scales differ between figures a, b and c. Acronyms: C (Control); CDM (Dry meadow community), CWM (Wet meadow community); F-DC (*Daucus carota*); F-GR (*Geum rivale*); G-DC (*Deschampsia cespitosa*); G-FO (*Festuca ovina*); L-LC (*Lotus corniculatus*) and L-LP (*Lotus pedunculatus*).

remove water, plant selection for resilient retention systems should consider water use efficiency under drought. This is important because projected increases in temperature, atmospheric CO_2 and drought due to climate change may differently affect contrasting plant functional types (e.g., C3 and C4 species) and their competitiveness (Sage and Kubien, 2003).

In the columns vegetated with the species mixes (i.e., CDM and CWM), water loss was greater than the average water loss from the three contrasting species in the mix. For instance, the total water loss from the dry meadow community was 28% greater than the expected average water loss from the three contrasting species (*D. carota*, *F. ovina* and *L. corniculatus*). Therefore, this represents an emergent property of the more biodiverse system, where more demanding and competitive species may optimize water use benefiting from less competition between diverse plants. In the case of the dry meadow community (CDM), *L. corniculatus* might have increased its transpiration compensating for the small water usage of *D. carota* and *F. ovina*. Encouragingly, based on our results, there is no tradeoff between engineering functionality and plant biodiversity as it is possible to enhance biodiversity without compromising the engineering services (e.g., water removal). Indeed, when all treatments (i.e., control soil; contrasting species; contrasting plant communities) are considered for key functions in bioretention systems such as hydraulic conductivity, water retention and evapotranspiration, plant community can be generally ranked in the three top positions for their performance (1stCWM for Ks (Fig. 1a); 3rd CWM for daily water loss (Fig. 2a); 2nd CWM for soil strength (Fig. 4); 1st CWM and 3rd CDM for soil PAW (Fig. 6d)). Similarly, a study by Lundholm (2015) on green roofs found that species mixtures can outperform monocultures for multiple ecosystem services including stormwater retention. Our results will contribute towards biodiverse plant selection for bioretention systems and hence the promotion of biodiversity in built environment. Indeed, functional advantage (i.e., service provisioning) of biodiversity may be desirable in constructed ecosystems also on cost grounds. Long-term, monospecific vegetation have generally a limited ability to adapt to environmental fluctuations and changes. Contrasting responses of diverse species to environmental factors (e.g., extreme climatic events or pests) contribute to ecosystem resilience, particularly in a changing environment and climate. In ecology, this has been explained using the concepts of functional redundancy and functional insurance (Diaz and Cabido, 2001). Functional redundancy makes systems more resilient, as several species may have similar function (e.g., ecosystem service). Functional insurance is determined by the functional richness, which increases the probability that some species will respond positively to a perturbation. Ideally, plant screening for long-term resilience of retention systems should identify different species with similar function (e.g., high transpiration) as well as species with different temporal and spatial responses to environmental perturbations (i.e., functional insurance). Functional diversity limiting interspecific competition may be more important for ecosystem resilience than simple species diversity (i.e., number of species) alone. The matric suction induced by soil drying differed greatly between treatments, soil depth and time (Fig. 3). While in the shallow soil, all species were able to induce large matric suction values, in the deeper soil layers (> 0.2 m) large matric suction values were recorded after a longer time period, and not all species were able to induce high values of matric suction (e.g., *F. ovina*). Differences in the induced matric suction down the soil profile appear to be the result of different root depths and densities in the soil vegetated with contrasting species. For instance, Figs. 9b and c show an exponential decrease in both root biomass and length down the soil profile of *F. ovina* columns. Our results are in contrast with the study by Ng et al. (2013), where the vertical influence zone of suction was up to four-times the root zone for the grass *C. dactylon*. However, it should be noted that the root zone in Ng et al. (2013) was only 50 mm deep and suction monitoring was limited to shallow soil (≈ 0.2 m). The low water uptake by *D. carota* (Figs. 2 and 3) can be explained by the poor development of fine roots for water uptake, while most of the biomass in the taproot has a storage function (Fig. 9). Similar observations on induced matric suction and root growth in depth have been reported for contrasting woody species by Boldrin et al. (2018). Knowing the root zone of influence in the soil (e.g., depth of plant water uptake) is key for optimizing species selection and the design of bioretention barriers. For example, planting species with a shallow root system on a thick bioretention barrier will result in an inefficient system, because water cannot be removed from the deeper soil layers and the water storage

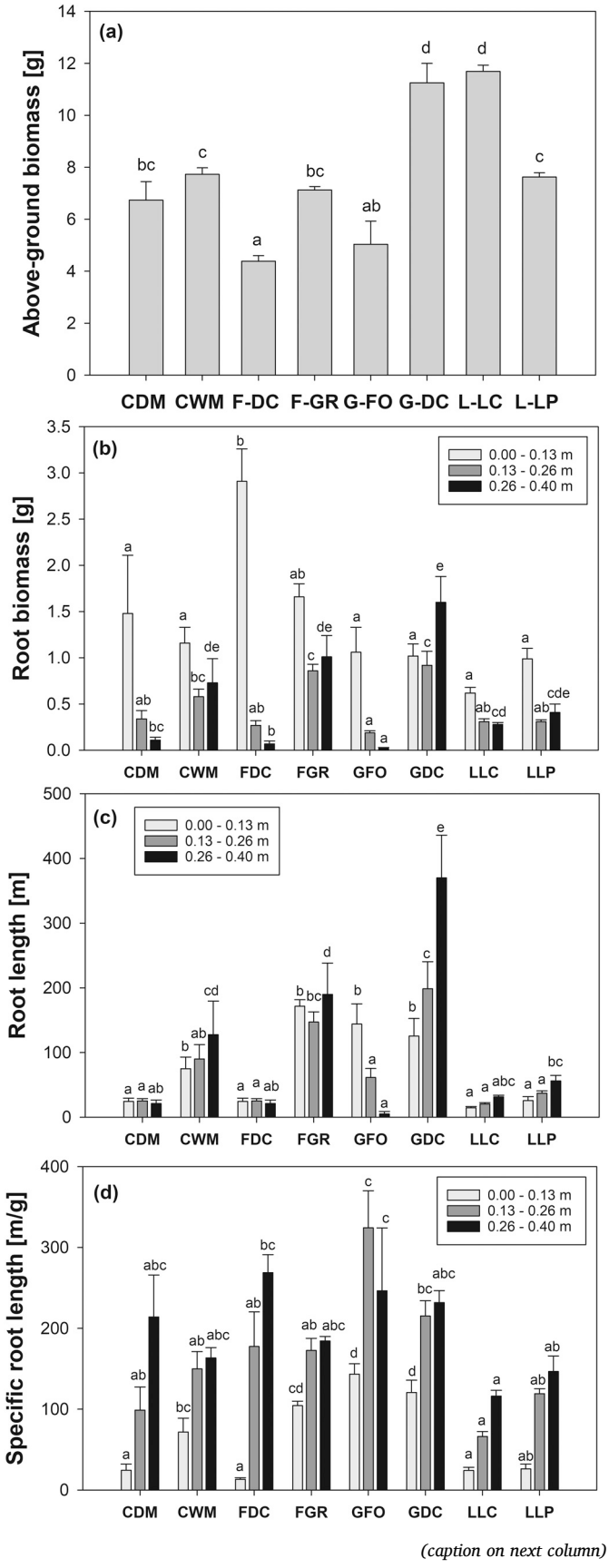

(caption on next column)

Fig. 9. (**a**) Above-ground biomass; (**b**) root biomass; (**c**) root length; and (**d**) specific root length measured down the soil profile (three depth ranges in soil columns). Means are reported ± standard error of mean ($n = 5$). Letters indicate a statistically significant difference between treatments, as tested using one-way ANOVA (p-value <0.001) followed by post hoc Tukey's test. Acronyms: C (Control); CDM (Dry meadow community), CWM (Wet meadow community); F-DC (*Daucus carota*); F-GR (*Geum rivale*); G-DC (*Deschampsia cespitosa*); G-FO (*Festuca ovina*); L-LC (*Lotus corniculatus*) and L-LP (*Lotus pedunculatus*).

capacity will be recharged only in the shallow rooted soil. Therefore, our results on water uptake and induced matric suction down the soil profile can assist species selection to implement efficient bioretention earth barrier systems.

4.3. Soil strength gain

Soil strength varied greatly between treatments during both wet (i.e., after saturation) and dry (after ET monitoring) conditions (Fig. 4). In particular, an abrupt strength gain was recorded after the drying period (e.g., up to 12-times in *L. corniculatus* soil). Indeed, the penetration resistance (i.e., soil strength) recorded after ET monitoring showed a positive correlation with daily evapotranspiration (Fig. 11b).

The strength gain upon drying was driven by the large values of matric suction (and hence effective stress) induced by plant water uptake (Figs. 2 and 3). Transpiration-induced suction has been recognised as one of the main reinforcement processes (increase in apparent cohesion) in soil to resist shearing (Simon and Collison, 2002). This soil reinforcement can play a major role in stabilising a water retention barrier on a slope (Leung et al., 2017; Rahardjo et al., 2014; Yildiz et al., 2019). Although after saturation the strength differences between control and vegetated columns were smaller compared to the values observed after ET, the strength gain of the vegetated soil during wet conditions (i.e., no suction effect) can be of greater interest for the stability of bioretention systems targeting flood mitigation. Soil vegetated with *D. carota* and *Lotus* spp. was more than 2.5-times stronger than the control soil. We hypothesise that this strength gain is the result of soil structural changes induced by root growth and water uptake (e.g., wetting-drying cycles) (Jin et al., 2017), as well as mobilisation of root tensile strength (also known as, root mechanical reinforcement) in the root-soil composite (Comino et al., 2010). In particular, the strength gain in the *D. carota* vegetated soil can be explained by soil densification induced by the radial growth of thick *C. carota* tap roots (Supplementary Fig. 4g–i) (Bruand et al., 1996). Changes in soil structure were also highlighted by the significantly greater wet aggregate stability in vegetated soil (Fig. 5) in agreement with the literature (Tisdall and Oades, 1979; Tisdall and Oades, 1982). The compression induced by root water uptake (e.g., wetting-drying cycles) forms aggregates that are denser and of greater strength than those in unvegetated soils (Jin et al., 2017). Moreover, exudates released by roots can increase aggregate stability (Angers and Caron, 1998), as well as soil hardness and elasticity (Naveed et al., 2018). For example, Naveed et al. (2018) showed an increase of both hardness and elasticity of sandy loam soil with increasing exudate concentration from both *Hordeum vulgare* and *Zea mays*. The intrusion of the roots of herbaceous species may also form a root-soil composite with enhance mechanical properties such as resistance in tension (Comino et al., 2010; Loades et al., 2010). Mechanical reinforcement differences between contrasting species, such as those tested in the present study, can be explained by root length density in soil, root-system architecture and root biomechanical properties (Boldrin et al., 2021; Comino et al., 2010; De Baets et al., 2008; Loades et al., 2010). For instance, Comino et al. (2010) reported a shear strength gain of 10.2 ± 3.4 kPa (% increase = 693) in soil vegetated with *L. corniculatus* when compared with fallow soil. Therefore, the large strength gain of soil vegetated with *L. corniculatus* in the present study could be explained by the mobilisation of soil-root interface friction and

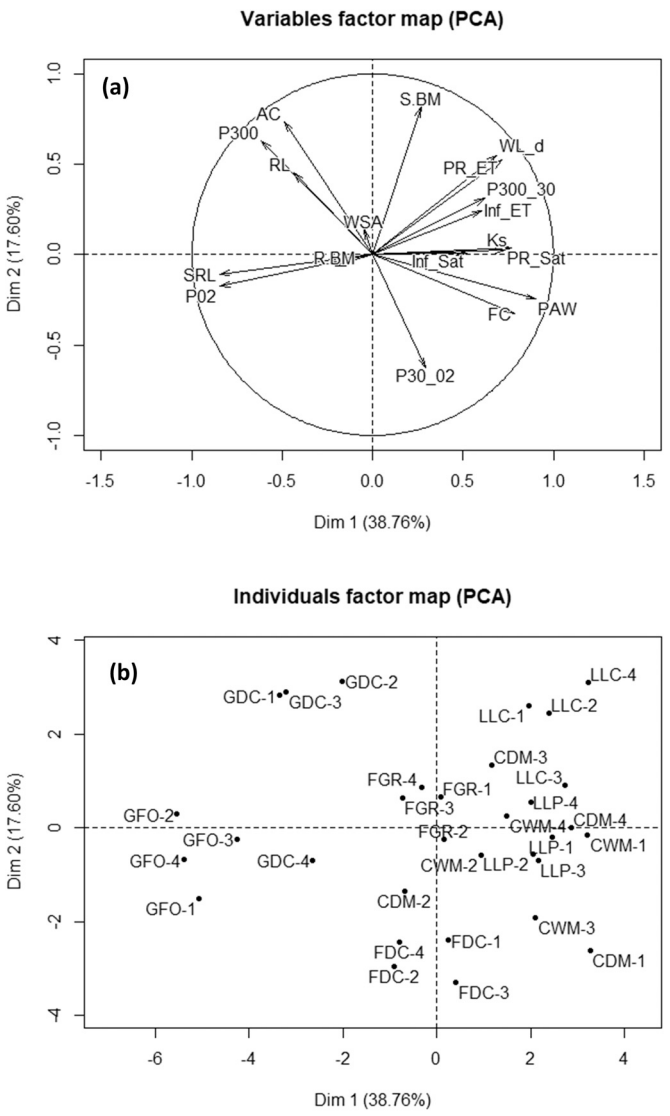

Fig. 10. Variables factor map (**a**) and individual factor map (**b**) of the principal component analysis (PCA) of plant traits and soil hydro-mechanical parameters on the plane represented by the first two dimensions of the principal component analysis (Dim1: 38.76% of variation; Dim2: 17.60% of variation). Acronyms of plant traits, soil parameters and treatments: S.BM (Shoot biomass, see Fig. 9a); R.BM (root biomass, see Fig. 9b); RL (root length, see Fig. 9c); SRL (average specific root length, see Fig. 9d); Ks (saturated hydraulic conductivity, see Fig. 1a); Inf_Sat (infiltration after saturation, see Fig. 1b); Inf_ET (infiltration after evapotranspiration period, see Fig. 1b); PR_Sat (penetration resistance at saturation, see Fig. 4); PR_ET (penetration resistance after evapotranspiration period, see Fig. 4); WL_d (daily evapotranspiration, see Fig. 2); FC (water content at field capacity of soil, see Fig. 6b); AC (air content at field capacity, see Fig. 6c); PAW (plant available water, see Fig. 6d); P0300 (pores with diameter > 300 μm, see Fig. 7); P300_30 (pores with diameter between 300 and 30 μm, see Fig. 7); P30_02 (pores with diameter between 30 and 0.2 μm, see Fig. 7); P02 (pores with diameter < 0.2 μm, see Fig. 7); WSA (water stable aggregates, see Fig. 5); CDM (Dry meadow community), CWM (Wet meadow community); FDC (*Daucus carota*); FGR (*Geum rivale*); GDC (*Deschampsia cespitosa*); GFO (*Festuca ovina*); LLC (*Lotus corniculatus*) and LLP (*Lotus pedunculatus*).

hence the root mechanical reinforcement (Fig. 4). However, it should be noted that in addition to this, soil strength gains driven by changes in soil structure (e.g., aggregate stability) could have also contributed to the penetration resistance differences after saturation.

In our study, aggregate stability was the greatest in the soil vegetated with *F. ovina*, where more than 30% of aggregates did not disperse in water. In contrast, less than 5% of aggregates were stable in the control soil (Fig. 5). The greatest number of stable aggregates in the *F. ovina* vegetated soil can be explained by its dense fibrous root system (Figs. 9c, d and Supplementary Fig. 3m–o). The increase of stable aggregates in soil vegetated with *F. ovina* further strengthens the argument for biodiverse vegetation incorporating several desirable functions: whilst other species outperformed *F. ovina* in terms of hydraulic conductivity (Fig. 1) and evapotranspiration (Fig. 2), *F. ovina* induced greater aggregates stability (Fig. 5). Indeed, fine roots are largely responsible for the improvement of soil aggregate stability (Pohl et al., 2012). Aggregate stability enhances soil resistance to erosion (Andreu et al., 2001), as well as soil porosity and hence hydraulic conductivity (Bronick and Lal, 2005). However, in our study we did not identify any clear relation between aggregate stability and soil hydrological or hydraulic properties. Longer time (e.g., several growing seasons) may be necessary to appreciate the gradual evolution of hydrological and hydraulic changes induced by soil aggregation, as well as significant species effects. Moreover, while K_s was tested on the entire soil volume, soil for aggregate stability was tested only for shallow soil. In a bioretention system (e.g., earth barrier system), soil stability and high K_s are desirable properties driving faster infiltration and a greater resistance to extreme climate events (e.g., less sediment washout in the drainage system).

4.4. Water retention properties

The relationships between soil water content and matric suction (aka soil water retention curves) varied between treatments (Fig. 6) and significant differences were found between water contents of different treatments equilibrated to the same matric suctions. Vegetated soil, with the exception of grass-vegetated soil, showed a significantly greater water content at field capacity (i.e., at 5 kPa; Fig. 6b). It is interesting to notice that species belonging to the same plant functional type showed similar and consistent effects on soil water retention properties. For instance, when we consider different parameters estimated from SWRCs (Fig. 6b,c,d), the soil vegetated with the two grass species (*D. cespitosa* and *F. ovina*) showed a small effect (i.e., values close to control soil) compared with other plant functional types (e.g., legumes). It should be noted that the two contrasting grasses clearly differ in plant traits (Fig. 9). The consistent lack of an effect in the grass-vegetated soil can be explained by the fibrous root system, where no thick roots are present (Supplementary Figs. 3m-r and 4m-r). Indeed, the intrusion of fine roots without radial growth (i.e., no secondary development) probably had little effect in terms of rhizosphere densification and loss of voids, while on the contrary soil particles are rearranged in stable aggregate by these dense fibrous roots-systems and their exudates (Fig. 5). In contrast with grasses, the air content at field capacity and the volume of aeration pores (Figs. 6c and 7) showed a remarkable drop in soil vegetated with plant communities and *D. carota*. The loss of macropores (e.g., aeration pores) in the soil vegetated with plant communities can be explained by a more efficient occupancy and manipulation of soil voids in a species mix, where contrasting root morphologies were present. Similarly, the large radial growth of *D. carota* tap roots (Supplementary Fig. 4g–i) might have resulted in a soil densification and hence loss of large voids, in agreement with the observations by Bruand et al. (1996) on rhizosphere soil. The densification of soil in the cores vegetated with *D. carota* and tested for SWRC is also supported by the greater penetration resistance compared to other treatments (Fig. 8a). The theoretical plant available water (PAW), estimated by SWRCs, was negatively correlated with specific root length (SRL) of contrasting species (Fig. 11 c). Therefore, soil colonised by fine and dense root systems (e.g., grasses) was associated with smaller values of PAW when compared with soils colonised by root systems characterised by thick and more diameter-heterogenous roots. This observation can be explained by the relative changes in the volume of macro- and mesopores storing available water, as well as changes of micropores storing unavailable water at permanent wilting point (see calculation of PAW in *Materials and Methods*). For instance,

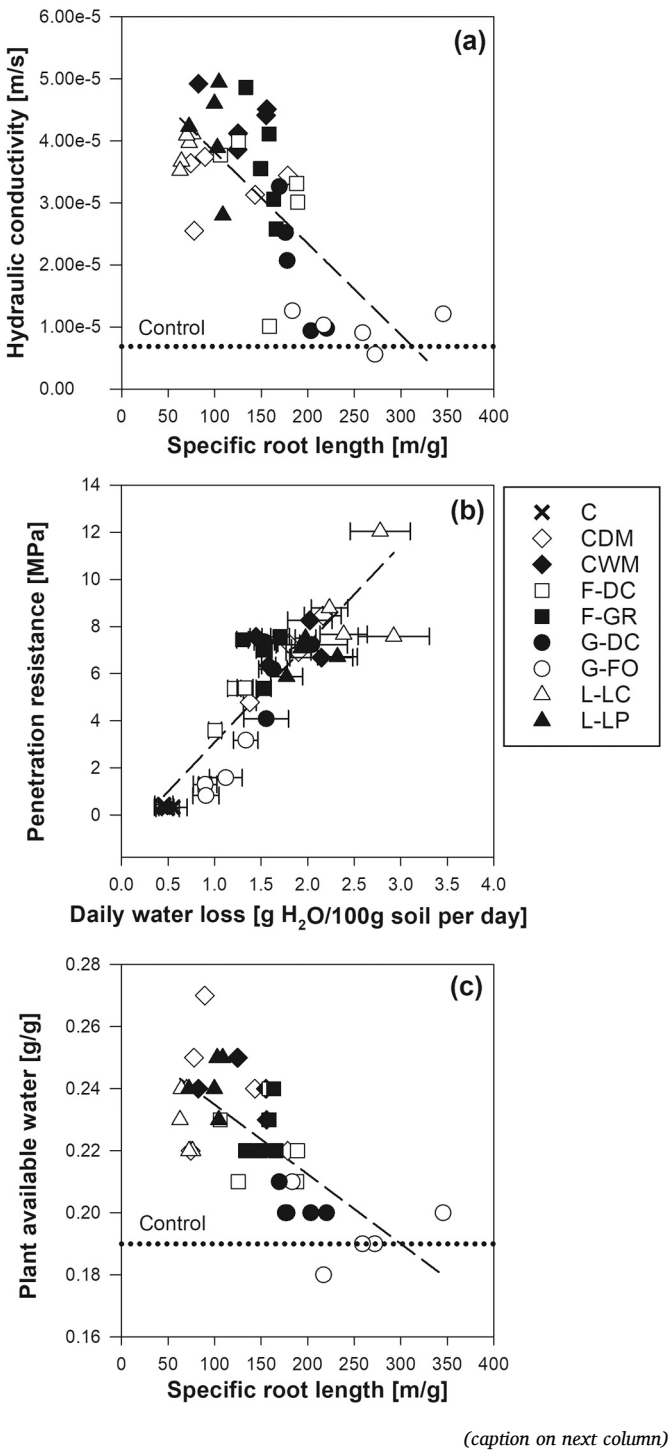

(caption on next column)

Fig. 11. Scatter plots of significant relationships identified in the PC Biplot (Fig. 10). (**a**) Correlation between average specific root length (*SRL*; see Fig. 9d) and saturated hydraulic conductivity (K_s; see Fig. 1a) (n = 5). Dashed line represents the linear regression model and trend of correlation [$K_s = -1.47e^{-7}*SRL + 5.29e^{-5}$; $R^2 = 0.52$; p-value<0.001]. Dotted line gives the average value recorded in control columns (fallow soil). (**b**) Correlation between average daily water loss (WL_d) and penetration resistance (*PR*; see Fig. 4) recorded after the water loss monitoring. Average daily water loss was calculated averaging the water loss between consecutive recordings (see Fig. 2) during the 21 days monitoring (n = 4). Dashed line represents the linear regression model and trend of correlation [$PR = 4.18*WL_d$-1.10; $R^2 = 0.77$; p-value<0.001]. Mean values of daily evapotranspiration are reported ± standard error of mean. (**c**) Correlation between average specific root length (*SRL*; see Fig. 9d) and plant available water (*PAW*; see Fig. 6d) (n = 5). Dashed line represents the linear regression model and trend of correlation [PAW = -2.00 $e^{-4}*SRL$ + 0.2572; $R^2 = 0.49$; p-value<0.001]. Dotted line gives the average value recorded in control columns (fallow soil). Acronyms: C (Control); CDM (Dry meadow community), CWM (Wet meadow community); F-DC (*Daucus carota*); F-GR (*Geum rivale*); G-DC (*Deschampsia cespitosa*); G-FO (*Festuca ovina*); L-LC (*Lotus corniculatus*) and L-LP (*Lotus pedunculatus*).

the increase of pores within the 30–0.2 μm diameter-class and the decrease of micropores smaller than 0.2 μm can translate in an overall increase of PAW.

The changes in water retention curves induced by roots have been rarely investigated in the literature, particularly when considering contrasting species. Our results (Fig. 6) are in agreement with previous observations by Leung et al. (2015b) on soil vegetated with a *Schefflera heptaphylla* tree. Leung et al. (2015a, 2015b) found greater matric suction (per given water content) in vegetated soil compared to fallow soil. Indeed, rhizosphere soil (small soil volume surrounding the root) has been shown to present distinct hydrological properties and dynamics compared to bulk soil (Bengough, 2012). Carminati et al. (2010) showed a distinct, hysteretic and time-dependent water retention curve of the rhizosphere soil. This water retention property changes with root ageing, facilitating water uptake (Carminati and Vetterlein, 2013). The distinct water retention properties of rhizosphere soil have been explained with soil structural changes (Koebernick et al., 2019; Whalley, 2005) and chemical properties of root exudates (Read et al., 2003). Therefore, it can be hypothesised that changes at rhizosphere scale can also influence the water retention properties of vegetated soil. Furthermore, although organic matter concentration did not differ between treatments (e.g., control and vegetated soil) after one growing season in this study (data not shown), it can be hypothesised that after several growing seasons and notable turnover of plant materials (litter and roots), organic matter can accumulate in soil to influence the water holding capacity. Indeed, in long-term, organic matter can have major effects on water retention properties of soils because of its effect on water holding capacity, hydrophobicity and the associate influence on soil structure (Tivet et al., 2013).

The estimated volume of pores with key functions for soil hydrology further highlighted consistent effects induced by plants belonging to the same plant functional type (Fig. 7). Grasses and legumes showed opposite trends in terms of the increase or decrease in pore volume (compared with control soil) when the pore-diameter classes “300 – 30 μm” and “< 0.2 μm” were considered. The fibrous root system of grasses had a small influence compared with other plant functional types (i.e., values close to the control soil). Furthermore, the differences in the volume of drainage pores (300–30 μm) between treatments showed similar trends to soil penetration resistance (Fig. 8a). This similarity supports the hypothesis that the observed differences in water retention properties resulted from structural more than chemical changes induced by root growth.

Coarse root systems have previously been found to increase soil macro-porosity by 30%, while species with dense fine root systems enhanced mesopore volume (Bodner et al., 2014). In contrast, our study did not find an increase in macropores in the presence of coarse roots (e.

g., soil vegetated with *D. carota*). Formation of macropores (e.g., aeration pores) might have been limited due to little root turnover (i.e., root decay) during a single growing season. Furthermore, the soil cores for SWRCs and porosity estimation (≈ 4% of soil column volume) might have been too small to represent the spatial heterogeneity of root channels and cracks. Indeed, the differences and variability of SWRCs (Fig. 6) were smaller compared to those of soil hydraulic conductivity (Fig. 1). Changes in soil structure and water retention properties induced by vegetation are generally ignored in the design and assessment of nature-based solutions (e.g., bioretention systems). However, our results highlight a significant vegetation effect on soil structure and retention properties, which may be included in future designs. Improving water retention of soil can enhance the system resilience against extreme weathers events by increasing both water holding capacity (resilience against intense rain events) and water availability for plants (i.e., resilience against drought). Indeed, climate change has already been leading to variable weather with increased frequency of both floods and droughts (Hanlon et al., 2021; Herring et al., 2018; IPCC, 2022; Rakovec et al., 2022).

5. Conclusions

This study highlighted and quantified multiple soil-plant interactions that can benefit soil bioengineering solutions, such as earth barrier systems for flood mitigation. The use of vegetation can provide several engineering and ecological services at the same time, in contrast with traditional engineering solutions. For instance, the hydraulic conductivity of vegetated soil was generally larger than that of control fallow soil. However, the tested species significantly differed in their effect. Interestingly, the legume *L. corniculatus* induced the greatest increase in hydraulic conductivity (compared to the control), as well as the fastest water removal rate by transpiration (i.e., recharging the storage capacity of soil). Furthermore, notable changes in soil structure (e.g., aggregate stability), strength (e.g., penetration resistance) and water retention (e.g., SWRCs) were found to vary in relation to plant functional type. The species mix (biodiverse vegetation) highlighted emergent properties such as a greater transpiration rate (i.e., water removal) compared with the simple average of single species in the mix. Therefore, biodiverse vegetation maximised both functionality and resilience of nature-based solutions.

This study focused on soil-plant interactions in soil columns maintained under controlled conditions (glasshouse) during one growing season (i.e., summer). Future work is needed to study these soil-plant interactions under full-scale bioretention systems for a range of soil types and for both summer and winter rainfall events. Indeed, service provisioning by vegetation depends on season (Boldrin et al., 2018). For example, water removal by transpiration can be small during autumn and winter due to plant dormancy and low vapor pressure deficit in the atmosphere. In the long-term, other factors, such as organic matter accumulation, can alter the water retention properties of vegetated soil. Furthermore, assessment of flood-mitigation by retention system should include climatic factors such as rainfall intensity, return period and the time before consecutive rain events. For instance, the water retention capacity of the barrier cannot be fully re-established if successive rain events occur in a short period of time, even if plants with high water-demand are used.

Declaration of Competing Interest

The authors declare that they have no known competing financial interests or personal relationships that could have appeared to influence the work reported in this paper.

Acknowledgements

This work was funded by the EPSRC project (EP/R005834/1) "Climate Adaptation Control Technologies for Urban Spaces (CACTUS)". The James Hutton Institute receives funding from the Rural & Environment Science & Analytical Services Division of the Scottish Government. The author (AKL) acknowledges the financial support provided by the GRF/16202720 and CRF/C6006-20G funded by the Hong Kong Research Grants Council as well as #51922112 provided by the National Natural Science Foundation of China (NSFC).

Appendix A. Supplementary data

Supplementary data to this article can be found online at https://doi.org/10.1016/j.ecoleng.2022.106668.

References

Andreu, V., Imeson, A.C., Rubio, J.L., 2001. Temporal changes in soil aggregates and water erosion after a wildfire in a Mediterranean pine forest. CATENA 44, 69–84. https://doi.org/10.1016/S0341-8162(00)00177-6.

Angers, D.A., Caron, J., 1998. Plant-induced changes in soil structure: Processes and feedbacks. In: Van Breemen, N. (Ed.), Plant-Induced Soil Changes: Processes and Feedbacks. Springer Netherlands, Dordrecht.

Archer, N.A.L., Bonell, M., Coles, N., MacDonald, A.M., Auton, C.A., Stevenson, R., 2013. Soil characteristics and landcover relationships on soil hydraulic conductivity at a hillslope scale: a view towards local flood management. J. Hydrol. 497, 208–222. https://doi.org/10.1016/j.jhydrol.2013.05.043.

Archer, N.A.L., Otten, W., Schmidt, S., Bengough, A.G., Shah, N., Bonell, M., 2015. Rainfall infiltration and soil hydrological characteristics below ancient forest, planted forest and grassland in a temperate northern climate. Ecohydrology. https://doi.org/10.1002/eco.1658.

Bastin, J.-F., Clark, E., Elliott, T., Hart, S., van den Hoogen, J., Hordijk, I., Ma, H., Majumder, S., Manoli, G., Maschler, J., Mo, L., Routh, D., Yu, K., Zohner, C.M., Crowther, T.W., 2019. Understanding climate change from a global analysis of city analogues. PLoS One 14, e0217592. https://doi.org/10.1371/journal.pone.0217592.

Bengough, A.G., 2012. Water dynamics of the root zone: Rhizosphere biophysics and its control on soil hydrology. Vadose Zone J. 11 https://doi.org/10.2136/vzj2011.0111.

Bodner, G., Leitner, D., Kaul, H.P., 2014. Coarse and fine root plants affect pore size distributions differently. Plant Soil 380, 133–151. https://doi.org/10.1007/s11104-014-2079-8.

Boldrin, D., Leung, A.K., Bengough, A.G., 2017. Correlating hydrologic reinforcement of vegetated soil with plant traits during establishment of woody perennials. Plant Soil 416, 437–451. https://doi.org/10.1007/s11104-017-3211-3.

Boldrin, D., Leung, A.K., Bengough, A., 2018. Hydrologic reinforcement induced by contrasting woody species during summer and winter. Plant Soil. https://doi.org/10.1007/s11104-018-3640-7.

Boldrin, D., Leung, A.K., Bengough, A.G., 2020. Hydro-mechanical reinforcement of contrasting woody species: a full-scale investigation of a field slope. Géotechnique 0, 1–15. https://doi.org/10.1680/jgeot.19.SiP.018.

Boldrin, D., Bengough, A.G., Lin, Z., Loades, K.W., 2021. Root age influences failure location in grass species during mechanical testing. Plant Soil. https://doi.org/10.1007/s11104-020-04824-6.

Bronick, C.J., Lal, R., 2005. Soil structure and management: a review. Geoderma 124, 3–22. https://doi.org/10.1016/j.geoderma.2004.03.005.

Bruand, A., Cousin, I., Nicoullaud, B., Duval, O., Bégon, J.C., 1996. Backscattered electron scanning images of soil porosity for analyzing soil compaction around roots. Soil Sci. Soc. Am. J. 60, 895–901.

Carminati, A., Vetterlein, D., 2013. Plasticity of rhizosphere hydraulic properties as a key for efficient utilization of scarce resources. Ann. Bot. 112, 277–290. https://doi.org/10.1093/aob/mcs262.

Carminati, A., Moradi, A.B., Vetterlein, D., Vontobel, P., Lehmann, E., Weller, U., Vogel, H.J., Oswald, S.E., 2010. Dynamics of soil water content in the rhizosphere. Plant Soil 332, 163–176. https://doi.org/10.1007/s11104-010-0283-8.

Chen, S.S., Tsang, D.C.W., He, M., Sun, Y., Lau, L.S.Y., Leung, R.W.M., Lau, E.S.C., Hou, D., Liu, A., Mohanty, S., 2021. Designing sustainable drainage systems in subtropical cities: challenges and opportunities. J. Clean. Prod. 280, 124418 https://doi.org/10.1016/j.jclepro.2020.124418.

CIRIA (Ed.), 2016. The SuDS manual (C753). In: CIRIA (ed).

Comino, E., Marengo, P., Rolli, V., 2010. Root reinforcement effect of different grass species: a comparison between experimental and models results. Soil Tillage Res. 110, 60–68. https://doi.org/10.1016/j.still.2010.06.006.

De Baets, S., Poesen, J., Knapen, A., Barbera, G.G., Navarro, J.A., 2007. Root characteristics of representative Mediterranean plant species and their erosion-reducing potential during concentrated runoff. Plant Soil 294, 169–183. https://doi.org/10.1007/s11104-007-9244-2.

De Baets, S., Poesen, J., Reubens, B., Wemans, K., De Baerdemaeker, J., Muys, B., 2008. Root tensile strength and root distribution of typical Mediterranean plant species and their contribution to soil shear strength. Plant Soil 305, 207–226. https://doi.org/10.1007/s11104-008-9553-0.

Diaz, S., Cabido, M., 2001. Vive la difference: plant functional diversity matters to ecosystem processes. Trends Ecol. Evol. 16, 646–655. https://doi.org/10.1016/s0169-5347(01)02283-2.

Ghestem, M., Sidle, R.C., Stokes, A., 2011. The influence of plant root systems on subsurface flow: Implications for slope stability. BioScience 61, 869–879. https://doi.org/10.1525/bio.2011.61.11.6.
Ghestem, M., Cao, K., Ma, W., Rowe, N., Leclerc, R., Gadenne, C., Stokes, A., 2014. A framework for identifying plant species to be used as 'ecological engineers' for fixing soil on unstable slopes. PLoS One 9. https://doi.org/10.1371/journal.pone.0095876.
Gimenez-Maranges, M., Breuste, J., Hof, A., 2020. Sustainable Drainage Systems for transitioning to sustainable urban flood management in the European Union: a review. J. Clean. Prod. 255, 120191 https://doi.org/10.1016/j.jclepro.2020.120191.
Gish, J.T., Jury, A.W., 1983. Effect of plant roots and root channels on solute transport. Trans. ASAE 26, 440–0444. https://doi.org/10.13031/2013.33955.
Greenland, D.J., 1981. Soil management and soil degradation. J. Soil Sci. 32, 301–322. https://doi.org/10.1111/j.1365-2389.1981.tb01708.x.
Greenwood, W.J., Buttle, J.M., 2014. Effects of reforestation on near-surface saturated hydraulic conductivity in a managed forest landscape, southern Ontario, Canada. Ecohydrology 7, 45–55. https://doi.org/10.1002/eco.1320.
Hanlon, H.M., Bernie, D., Carigi, G., Lowe, J.A., 2021. Future changes to high impact weather in the UK. Clim. Chang. 166, 50. https://doi.org/10.1007/s10584-021-03100-5.
Herring, S.C., Christidis, N., Hoell, A., Kossin, J.P., Schreck, C.J., Stott, P.A., 2018. Explaining extreme events of 2016 from a climate perspective. Bull. Am. Meteorol. Soc. 99, S1–S157. https://doi.org/10.1175/BAMS-ExplainingExtremeEvents2016.1.
Hill, M.O., 1999. Ellenberg's Indicator Values for British Plants. Institute of Terrestrial Ecology.
IPCC, 2013. Climate Change 2013: The Physical Science Basis. Contribution of Working Group I to the Fifth Assessment Report of the Intergovern¬Mental Panel on Climate Change 1535.
IPCC, 2022. Climate change 2022: impacts, adaptation, and vulnerability. In: Contribution of Working Group II to the Sixth Assessment Report of the Intergovernmental Panel on Climate Change.
Jiang, C., Li, J., Li, H., Li, Y., Chen, L., 2017. Field performance of bioretention systems for runoff quantity regulation and pollutant removal. Water Air Soil Pollut. 228, 468. https://doi.org/10.1007/s11270-017-3636-6.
Jin, K., White, P.J., Whalley, W.R., Shen, J., Shi, L., 2017. Shaping an optimal soil by root–soil interaction. Trends Plant Sci. 22, 823–829. https://doi.org/10.1016/j.tplants.2017.07.008.
Jotisankasa, A., Sirirattanachat, T., 2017. Effects of grass roots on soil-water retention curve and permeability function. Can. Geotech. J. 54, 1612–1622. https://doi.org/10.1139/cgj-2016-0281.
Koebernick, N., Daly, K.R., Keyes, S.D., Bengough, A.G., Brown, L.K., Cooper, L.J., George, T.S., Hallett, P.D., Naveed, M., Raffan, A., Roose, T., 2019. Imaging microstructure of the barley rhizosphere: particle packing and root hair influences. New Phytol. 221, 1878–1889. https://doi.org/10.1111/nph.15516.
Kovats, R.S., Valentini, R., Bouwer, L.M., Georgopoulou, E., Jacob, D., Martin, E., Rounsevell, M., Sous, J.-F., 2014. Europe. In: Climate change 2014: impacts, adaptation, and vulnerability. Part B: regional aspects. In: Barros, V.R., Field, C.B., Dokken, D.J., Mastrandrea, M.D., Mach, K.J., Bilir, T.E., Chatterjee, M., Ebi, K.L., Estrada, Y.O., Genova, R.C., Girma, B., Kissel, E.S., Levy, A.N., MacCracken, S., Mastrandrea, P.R., White, L.L. (Eds.), Contribution of Working Group II to the Fifth Assessment Report of the Intergovernmental Panel on Climate Change. Cambridge University Press, Cambridge, United Kingdom and New York, NY, USA.
Lambers, H., Chapin, F.S., Pons, T.L., 2008. Plant Physiological Ecology.
Leung, A.K., Garg, A., Coo, J.L., Ng, C.W.W., Hau, B.C.H., 2015a. Effects of the roots of Cynodon dactylon and Schefflera heptaphylla on water infiltration rate and soil hydraulic conductivity. Hydrol. Process. 29, 3342–3354. https://doi.org/10.1002/hyp.10452.
Leung, A.K., Garg, A., Ng, C.W.W., 2015b. Effects of plant roots on soil-water retention and induced suction in vegetated soil. Eng. Geol. 193, 183–197. https://doi.org/10.1016/j.enggeo.2015.04.017.
Leung, A.K., Kamchoom, V., Ng, C.W.W., 2017. Influences of root-induced soil suction and root geometry on slope stability: a centrifuge study. Can. Geotech. J. 54, 291–303. https://doi.org/10.1139/cgj-2015-0263.
Leung, A.K., Boldrin, D., Liang, T., Wu, Z.Y., Kamchoom, V., Bengough, A.G., 2018. Plant age effects on soil infiltration rate during early plant establishment. Géotechnique 68, 646–652. https://doi.org/10.1680/jgeot.17.T.037.
Liang, T., Bengough, A.G., Knappett, J.A., MuirWood, D., Loades, K.W., Hallett, P.D., Boldrin, D., Leung, A.K., Meijer, G.J., 2017. Scaling of the reinforcement of soil slopes by living plants in a geotechnical centrifuge. Ecol. Eng. https://doi.org/10.1016/j.ecoleng.2017.06.067.
Loades, K.W., Bengough, A.G., Bransby, M.F., Hallett, P.D., 2010. Planting density influence on fibrous root reinforcement of soils. Ecol. Eng. 36, 276–284. https://doi.org/10.1016/j.ecoleng.2009.02.005.
Lundholm, J.T., 2015. Green roof plant species diversity improves ecosystem multifunctionality. J. Appl. Ecol. 52, 726–734. https://doi.org/10.1111/1365-2664.12425.
Marzluff, J., Shulenberger, E., Endlicher, W., Alberti, M., Bradley, G., Ryan, C., Zum Brunnen, C., Simon, U., 2008. Urban Ecology: An International Perspective on the Interaction between Humans and Nature. Springer, US.
Mickovski, S.B., Hallett, P.D., Bransby, M.F., Davies, M.C.R., Sonnenberg, R., Bengough, A.G., 2009. Mechanical Reinforcement of Soil by Willow Roots: Impacts of root Properties and root failure Mechanism. Soil Sci. Soc. Am. J. 73, 1276–1285. https://doi.org/10.2136/sssaj2008.0172.
Misra, R.K., Li, F.D., 1996. The effects of radial soil confinement and probe diameter on penetrometer resistance. Soil Tillage Res. 38, 59–69. https://doi.org/10.1016/0167-1987(96)01022-7.
Naveed, M., Brown, L.K., Raffan, A.C., George, T.S., Bengough, A.G., Roose, T., Sinclair, I., Koebernick, N., Cooper, L., Hallett, P.D., 2018. Rhizosphere-scale quantification of hydraulic and mechanical properties of soil impacted by root and seed exudates. Vadose Zone J. 17 https://doi.org/10.2136/vzj2017.04.0083.
Ng, C.W.W., Woon, K.X., Leung, A.K., Chu, L.M., 2013. Experimental investigation of induced suction distribution in a grass-covered soil. Ecol. Eng. 52, 219–223. https://doi.org/10.1016/j.ecoleng.2012.11.013.
Ng, C.W.W., Ni, J.J., Leung, A.K., 2020. Effects of plant growth and spacing on soil hydrological changes: a field study. Géotechnique 70, 867–881. https://doi.org/10.1680/jgeot.18.P.207.
Ni, J.J., Leung, A.K., Ng, C.W.W., 2019. Modelling effects of root growth and decay on soil water retention and permeability. Can. Geotech. J. 56, 1049–1055. https://doi.org/10.1139/cgj-2018-0402.
Pagès, L., 2011. Root system architecture: analysis from root systems to individual roots. In: Gliński, J., Horabik, J., Lipiec, J. (Eds.), Encyclopedia of Agrophysics. Springer Netherlands, Dordrecht.
Petalas, A.L., Tsiampousi, A., Zdravkovic, L., Potts, D.M., 2021. Numerical investigation of the performance of engineered barriers in reducing flood risk. MATEC Web. Conf. 337, 04003.
Pohl, M., Graf, F., Buttler, A., Rixen, C., 2012. The relationship between plant species richness and soil aggregate stability can depend on disturbance. Plant Soil 355, 87–102. https://doi.org/10.1007/s11104-011-1083-5.
Pollen-Bankhead, N., Simon, A., 2010. Hydrologic and hydraulic effects of riparian root networks on streambank stability: is mechanical root-reinforcement the whole story? Geomorphology 116, 353–362. https://doi.org/10.1016/j.geomorph.2009.11.013.
Poorter, H., Bühler, J., van Dusschoten, D., Climent, J., Postma, J.A., 2012. Pot size matters: a meta-analysis of the effects of rooting volume on plant growth. Funct. Plant Biol. 39, 839–850. https://doi.org/10.1071/FP12049.
Rahardjo, H., Satyanaga, A., Leong, E.C., Santoso, V.A., Ng, Y.S., 2014. Performance of an instrumented slope covered with shrubs and deep-rooted grass. Soils Found. 54, 417–425. https://doi.org/10.1016/j.sandf.2014.04.010.
Rakovec, O., Samaniego, L., Hari, V., Markonis, Y., Moravec, V., Thober, S., Hanel, M., Kumar, R., 2022. The 2018–2020 multi-year drought sets a new benchmark in Europe. Earth's Future 10, e2021EF002394. https://doi.org/10.1029/2021EF002394.
Read, D.B., Bengough, A.G., Gregory, P.J., Crawford, J.W., Robinson, D., Scrimgeour, C. M., Young, I.M., Zhang, K., Zhang, X., 2003. Plant roots release phospholipid surfactants that modify the physical and chemical properties of soil. New Phytol. 157, 315–326. https://doi.org/10.1046/j.1469-8137.2003.00665.x.
Rummukainen, M., 2012. Changes in climate and weather extremes in the 21st century. WIREs Clim. Change 3, 115–129. https://doi.org/10.1002/wcc.160.
Sage, R.F., Kubien, D.S., 2003. Quo vadis C4? An ecophysiological perspective on global change and the future of C4 plants. Photosynth. Res. 77, 209–225. https://doi.org/10.1023/A:1025882003661.
Semadeni-Davies, A., Hernebring, C., Svensson, G., Gustafsson, L.-G., 2008. The impacts of climate change and urbanisation on drainage in Helsingborg, Sweden: Suburban stormwater. J. Hydrol. 350, 114–125. https://doi.org/10.1016/j.jhydrol.2007.11.006.
Seyedabadi, M.R., Eicker, U., Karimi, S., 2021. Plant selection for green roofs and their impact on carbon sequestration and the building carbon footprint. Environ. Challenge. 4, 100119 https://doi.org/10.1016/j.envc.2021.100119.
Simon, A., Collison, A.J.C., 2002. Quantifying the mechanical and hydrologic effects of riparian vegetation on streambank stability. Earth Surf. Process. Landf. 27, 527–546. https://doi.org/10.1002/esp.325.
Song, L., Li, J.H., Zhou, T., Fredlund, D.G., 2017. Experimental study on unsaturated hydraulic properties of vegetated soil. Ecol. Eng. 103, 207–216. https://doi.org/10.1016/j.ecoleng.2017.04.013.
Tang, A.M., Hughes, P.N., Dijkstra, T.A., Askarinejad, A., Brenčič, M., Cui, Y.J., Diez, J.J., Firgi, T., Gajewska, B., Gentile, F., Grossi, G., Jommi, C., Kehagia, F., Koda, E, TerMaat, H.W., Lenart, S, Lourenco, S., Oliveira, M., Osinski, P., Springman, S.M., Stirling, R., Toll, D.G., Van Beek, V., 2018. Atmosphere-vegetation-soil interactions in a climate change context; Impact of changing conditions on engineered transport infrastructure slopes in Europe. Quart. J. Eng. Geol. Hydrogeol. https://doi.org/10.1144/qjegh2017-103.
Tisdall, J., Oades, J., 1979. Stabilization of soil aggregates by the root systems of ryegrass. Soil Res. 17, 429–441. https://doi.org/10.1071/SR9790429.
Tisdall, J.M., Oades, J.M., 1982. Organic matter and water-stable aggregates in soils. J. Soil Sci. 33, 141–163. https://doi.org/10.1111/j.1365-2389.1982.tb01755.x.
Tivet, F., Sa, J.C.M., Lal, R., Briedis, C., Borszowskei, P.R., Santos, Jbd, Farias, A., Eurich, G.E., Hartman, DdC, Junior, M.N., Bouzinac, S., Séguy, L., 2013. Aggregate C depletion by plowing and its restoration by diverse biomass-C inputs under no-till in sub-tropical and tropical regions of Brazil. Soil Tillage Res. 126, 203–218.

Vergani, C., Graf, F., 2016. Soil permeability, aggregate stability and root growth: a pot experiment from a soil bioengineering perspective. Ecohydrology 9, 830–842. https://doi.org/10.1002/eco.1686.

Wei, Z., Yoshimura, K., Wang, L., Miralles, D.G., Jasechko, S., Lee, X., 2017. Revisiting the contribution of transpiration to global terrestrial evapotranspiration. Geophys. Res. Lett. 44, 2792–2801. https://doi.org/10.1002/2016GL072235.

Whalley, W.R., 2005. Structural differences between bulk and rhizosphere soil. Eur. J. Soil Sci. 56, 353–360. -2005 v.2056 no.2003. https://doi.org/10.1111/j.1365-2389.2004.00670.x.

Yildiz, A., Graf, F., Rickli, C., Springman, S.M., 2019. Assessment of plant-induced suction and its effects on the shear strength of rooted soils. Proc. Inst. Civil Eng. - Geotech. Eng. 172, 507–519. https://doi.org/10.1680/jgeen.18.00209.